Uniform enclosures for the phase and zeros of Bessel functions and their derivatives

Nikolay Filonov Michael Levitin Iosif Polterovich David A. Sher

arXiv:2402.06956v2; 26 February 2024

Abstract

We prove explicit uniform two-sided bounds for the phase functions of Bessel functions and of their derivatives. As a consequence, we obtain new enclosures for the zeros of Bessel functions and their derivatives in terms of inverse values of some elementary functions. These bounds are valid, with a few exceptions, for all zeros and all Bessel functions with non-negative indices. We provide numerical evidence showing that our bounds either improve or closely match the best previously known ones.

Contents

The accompanying `Mathematica` script and its printout are available for download at https://michaellevitin.net/bessels.html.

MSC(2020): Primary 33C10. Secondary 33F05, 34B30, 65D20.

Keywords: Bessel functions, Bessel zeros, phase function, Sturm oscillation theorem, one-dimensional Schrödinger equation

N. F.: St. Petersburg Department of Steklov Institute of Mathematics of RAS, Fontanka 27, 191023, St.Petersburg, Russia; St. Petersburg State University, University emb. 7/9, 199034, St.Petersburg, Russia; filonov@pdmi.ras.ru

M. L.: Department of Mathematics and Statistics, University of Reading, Pepper Lane, Whiteknights, Reading RG6 6AX, UK; M.Levitin@reading.ac.uk; https://www.michaellevitin.net

I. P.: Département de mathématiques et de statistique, Université de Montréal, CP 6128 succ Centre-Ville, Montréal QC H3C 3J7, Canada; iossif@dms.umontreal.ca; https://www.dms.umontreal.ca/~iossif

D. A. S.: Department of Mathematical Sciences, DePaul University, 2320 N. Kenmore Ave, 60614, Chicago, IL, USA; dsher@depaul.edu

§1. Introduction and main results

§1.1. Setup I: Bessel functions

Throughout,

$$J_\nu(x), \qquad Y_\nu(x)$$

are standard Bessel functions with $\nu \geq 0$, and

$$j_{\nu,k}, \qquad y_{\nu,k}$$

are their kth largest positive zeros, respectively, where $k \in \mathbb{N}$.

We further define

$$\mathscr{C}_{\nu,\tau}(x) := J_\nu(x)\cos(\pi\tau) + Y_\nu(x)\sin(\pi\tau),$$

where we choose the additional parameter $\tau \in (0, 1]$ for definiteness, see Figure 1. Note that

$$J_\nu(x) = -\mathscr{C}_{\nu,1}(x), \qquad Y_\nu(x) = \mathscr{C}_{\nu,\frac{1}{2}}(x).$$

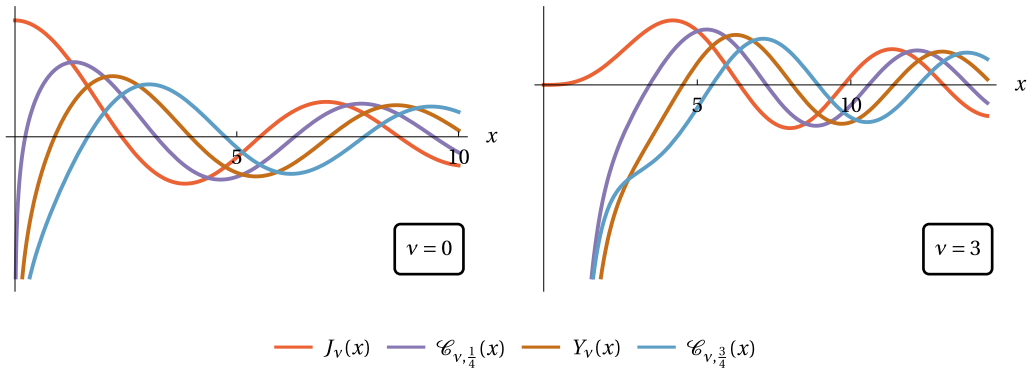

Figure 1: Plots of $\mathscr{C}_{\nu,\tau}(x)$.

We also introduce the Bessel *modulus* and *phase functions* $M_\nu, \theta_\nu : (0,+\infty) \to \mathbb{R}$ defined by

$$M_\nu(x) = \sqrt{J_\nu^2(x) + Y_\nu^2(x)}, \qquad J_\nu(x) + \mathrm{i} Y_\nu(x) = M_\nu(x)\left(\cos\theta_\nu(x) + \mathrm{i}\sin\theta_\nu(x)\right),$$

where we choose a continuous branch of $\theta_\nu(x)$ with the initial condition

$$\lim_{x\to 0^+} \theta_\nu(x) = -\frac{\pi}{2}.$$

For more details on the modulus and phase functions see [DLMF, §10.18] and [Ho17].

The following properties of the Bessel zeros and the modulus and phase functions are standard. We have

$$\nu < y_{\nu,1} < j_{\nu,1} < y_{\nu,2} < j_{\nu,2} < \dots < y_{\nu,k} < j_{\nu,k} < \dots,$$

see also [PA11] for further interlacing properties. Also,

$$M_\nu(x) > 0, \qquad \theta_\nu'(x) > 0 \qquad \text{for all } x > 0,$$

which means that the inverse function

$$\theta_\nu^{-1} : \left[-\frac{\pi}{2}, +\infty\right) \to [0,+\infty)$$

is well-defined and continuous. We also have, by [DLMF, (10.18.18)], the asymptotics

$$\theta_\nu(x) = x - \frac{\pi}{4}(2\nu+1) + \frac{4\nu^2-1}{8x} + \frac{(4\nu^2-1)(4\nu^2-25)}{384x^3} + O\left(x^{-5}\right) \qquad \text{as } x \to +\infty. \tag{1.1}$$

We have, since $j_{\nu,k}$ are the positive zeros of $\cos\theta_\nu(x)$, and $y_{\nu,k}$ are the positive zeros of $\sin\theta_\nu(x)$, the relations

$$j_{\nu,k} = \theta_\nu^{-1}\left(\pi\left(k - \frac{1}{2}\right)\right), \qquad y_{\nu,k} = \theta_\nu^{-1}\left(\pi(k-1)\right), \qquad k \in \mathbb{N}. \tag{1.2}$$

Some typical plots of functions θ_ν are shown in Figure 2.

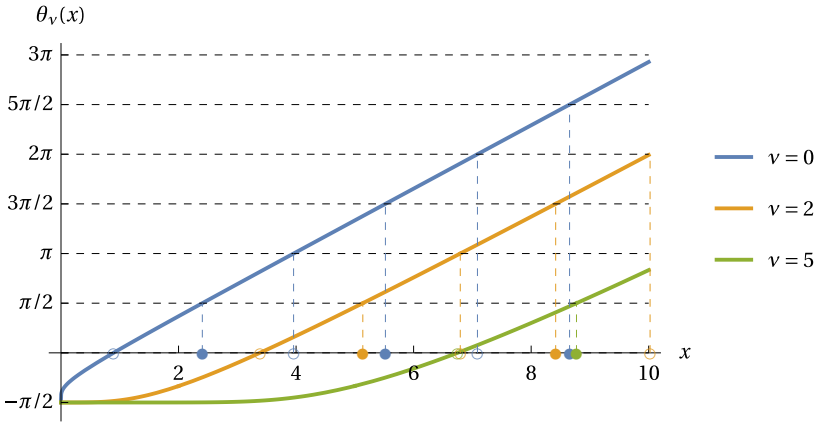

Figure 2: Plots of $\theta_\nu(x)$. The filled colour-coded dots on the horizontal axis indicate the positions of zeros $j_{\nu,k}$ and the hollow dots the positions of zeros $y_{\nu,k}$. The phase functions are calculated using the method of [Ho17].

We also have

$$\mathscr{C}_{\nu,\tau}(x) = M_\nu(x)\cos\left(\theta_\nu(x) - \pi\tau\right).$$

The kth positive zero of this function, which we will denote by $c_{\nu,\tau,k}$, is given by

$$c_{\nu,\tau,k} = \theta_\nu^{-1}\left(\pi\left(\tau + k - \frac{3}{2}\right)\right). \tag{1.3}$$

Remark 1.1. We know that the first zero of either $J_\nu(x)$ or $Y_\nu(x)$ is always bigger that ν. This is not necessarily the case for $c_{\nu,\tau,1}$ with $\tau \in \left(0, \frac{1}{2}\right)$. Indeed, we have

$$c_{\nu,\tau,1} = \theta_\nu^{-1}\left(\pi\left(\tau - \frac{1}{2}\right)\right) \leq \nu$$

whenever

$$0 < \tau \leq \tau_\nu^* := \frac{1}{\pi}\theta_\nu(\nu) + \frac{1}{2}.$$

Since $\theta_\nu(\nu) \in \left[-\frac{\pi}{2}, 0\right)$, we always have $\tau_\nu^* \in \left[0, \frac{1}{2}\right)$, see Figure 3. ◀

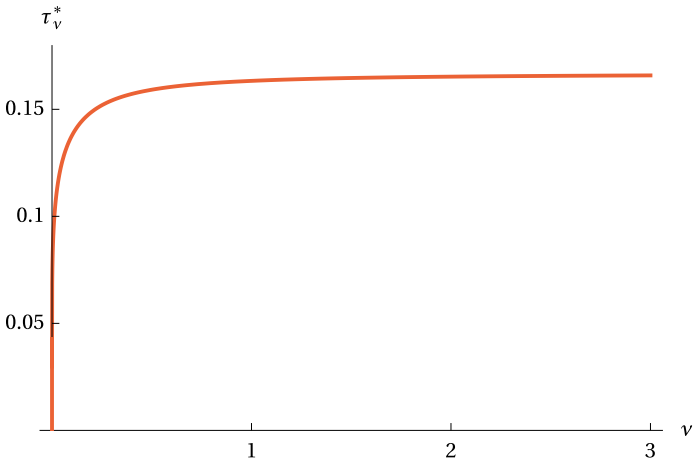

Figure 3: Plot of τ_ν^* against ν.

For further use, we additionally define the *counting function* of Bessel zeros,

$$\mathcal{N}_{J_\nu}(\lambda) := \#\left\{k \in \mathbb{N} : j_{\nu,k} \leq \lambda\right\}. \tag{1.4}$$

§1.2. Setup II: derivatives of Bessel functions

Consider, for $\nu \geq 0$, the derivatives of the Bessel functions

$$J_\nu'(x), \qquad Y_\nu'(x).$$

The numbers

$$j_{\nu,k}', \qquad y_{\nu,k}'$$

are their kth largest positive zeros except when $\nu = 0$, in which case we set

$$j_{0,1}' := 0.$$

We also consider the linear combinations

$$\mathscr{C}_{\nu,\tau}'(x) := J_\nu'(x)\cos(\pi\tau) + Y_\nu'(x)\sin(\pi\tau),$$

this time with $\tau \in [0, 1)$, see Figure 4.

As for the Bessel functions themselves, we also introduce the *modulus* and *phase functions* of the Bessel derivatives, $N_\nu, \varphi_\nu : (0, +\infty) \to \mathbb{R}$ defined by

$$N_\nu(x) = \sqrt{\left(J_\nu'(x)\right)^2 + \left(Y_\nu'(x)\right)^2}, \qquad J_\nu'(x) + \mathrm{i}Y_\nu'(x) = N_\nu(x)\left(\cos\varphi_\nu(x) + \mathrm{i}\sin\varphi_\nu(x)\right),$$

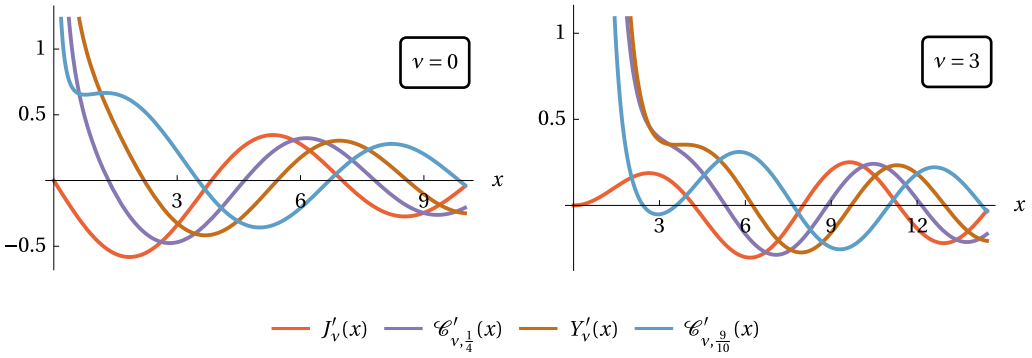

Figure 4: Plots of $\mathscr{C}'_{\nu,\tau}(x)$.

where we choose a continuous branch of $\varphi_\nu(x)$ with the initial condition

$$\lim_{x\to 0^+} \varphi_\nu(x) = \frac{\pi}{2},$$

see [DLMF, §10.18] and [Ho17].

The following properties of the Bessel derivatives zeros and the modulus and phase functions are standard:

$$\nu \le j'_{\nu,1} < y'_{\nu,1} < j'_{\nu,2} < y'_{\nu,2} < \dots < j'_{\nu,k} < y'_{\nu,k} < \dots$$

(with equality only for $\nu = 0$);

$$N_\nu(x) > 0 \qquad \text{for all } x > 0.$$

The phase function φ_ν is not monotone (except for $\nu = 0$) but has a single minimum at $x = \nu$, with $\varphi_\nu(\nu) \in \left(0, \frac{\pi}{2}\right)$ for $\nu > 0$. This means that its inverse function may only be defined on $[\varphi_\nu(\nu), +\infty)$; it is however easier to further restrict its domain and treat it as the function

$$\varphi_\nu^{-1} : \left[\frac{\pi}{2}, +\infty\right) \to [j'_{\nu,1}, +\infty).$$

Additionally, by [DLMF, (10.18.21)],

$$\varphi_\nu(x) = x - \frac{\pi}{4}(2\nu+1) + \frac{4\nu^2+3}{8x} + \frac{16\nu^4+184\nu^2-63}{384x^3} + O\left(x^{-5}\right) \qquad \text{as } x \to +\infty. \tag{1.5}$$

We have

$$j'_{\nu,k} = \varphi_\nu^{-1}\left(\pi\left(k - \frac{1}{2}\right)\right), \qquad y'_{\nu,k} = \varphi_\nu^{-1}(\pi k), \qquad k \in \mathbb{N}. \tag{1.6}$$

Further, let

$$c'_{\nu,\tau,k} :== \varphi_\nu^{-1}\left(\pi\left(\tau + k - \frac{1}{2}\right)\right), \qquad k \in \mathbb{N}, \tag{1.7}$$

be the kth largest zero of

$$\mathscr{C}'_{\nu,\tau}(x) = N_\nu(x)\cos\left(\varphi_\nu(x) - \pi\tau\right).$$

in the interval $\left[j'_{\nu,1}, +\infty\right)$.

Example 1.2. Our choice of enumeration of $c'_{\nu,\tau,k}$ means that we may disregard some positive zeros of $\mathscr{C}'_{\nu,t}$ below $j'_{\nu,1}$. For example, the right-hand side plot in Figure 4 shows that there are two zeros of $\mathscr{C}'_{3,\frac{9}{10}}$ below the first zero of J'_3, which are therefore excluded. ◀

Some typical plots of functions φ_ν are shown in Figure 5.

Similarly to (1.4), we also define the *counting function* of zeros of Bessel derivatives,

$$\mathscr{N}_{J'_\nu}(\lambda) := \#\left\{k \in \mathbb{N} : j'_{\nu,k} \le \lambda\right\}. \tag{1.8}$$

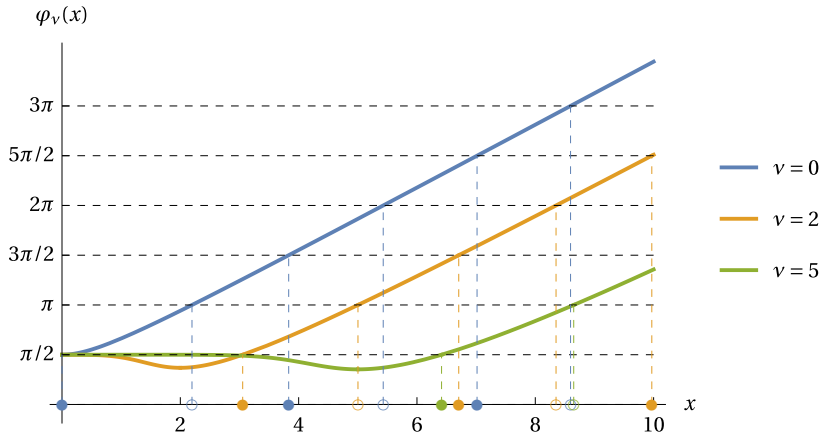

Figure 5: Plots of $\varphi_\nu(x)$. The filled colour-coded dots on the horizontal axis indicate the positions of zeros $j'_{\nu,k}$ and the hollow dots the positions of zeros $y'_{\nu,k}$. The phase functions are calculated using the method of [H017].

§1.3. Our philosophy and some history

The main purpose of our paper is to present new uniform (in ν) two-sided bounds for the phase functions $\theta_\nu(x)$ and $\varphi_\nu(x)$ (Theorems 1.4 and 1.10), and, as a consequence, new bounds for the zeros of Bessel functions and their derivatives (Corollaries 1.6 and 1.12) valid, with minimal exceptions, for all ν and k. Our bounds for the phase functions are expressed in terms of explicit elementary functions defined in §1.4 and §1.6, and the bounds for the zeros in terms of inverses of these functions. Additionally, due to the elementary nature of our bounds for phase functions, we derive simple bounds for the counting functions of zeros of Bessel functions and their derivatives (Corollaries 1.7 and 1.13), some of which have already been used to great effect in spectral-geometric problems, see [FLPS23] and [FLPS23a].

The common feature of our bounds and pre-existing bounds on zeros of Bessel functions and of their derivatives is that they are all based, in one form or another, on asymptotics of Bessel functions for large argument and/or order. We recall that there are, roughly speaking, three relevant asymptotic regimes, see [DLMF, §§10.17, 10.19–20]:

- ($\mathrm{R_i}$) the large-argument region, in which x approaches infinity and ν is fixed (or at least bounded);
- ($\mathrm{R_{ii}}$) the transition region, in which ν approaches infinity with $x \sim \nu + a\nu^{1/3}$ for some $a \in \mathbb{R}$. In this region the Bessel functions exhibit Airy-type behaviour;
- ($\mathrm{R_{iii}}$) the Debye expansion region, in which ν approaches infinity with $x \sim c\nu$ for some $c > 1$.

For a modern perspective on the interplay between these regimes, see [S23].

The general previously used approach to bounding Bessel zeros is essentially based on using the asymptotics of Bessel zeros in either of the regimes ($\mathrm{R_i}$) or ($\mathrm{R_{ii}}$), and then applying a form of the Sturm comparison theorem. Some existing bounds for the zeros of Bessel functions obtained using the expansions in the large argument regime ($\mathrm{R_i}$) are due to Hethcote [He70] and Elbert–Laforgia [EL00], see also [GG00, GG07, N21]. The explicit expressions of these bounds, which we use for benchmarking purposes, are collected in §4. Note that the lower bounds for Bessel zeros obtained in this way are only available for very low values of ν. Alternative bounds, based on the asymptotics of $j_{\nu,k}$ in the transitional regime ($\mathrm{R_{ii}}$), are given by Qu and Wong [QW96], and are also presented in §4. There is significantly less information in the literature on uniform bounds for the zeros $j'_{\nu,k}$ of derivatives of Bessel functions: we failed to find any bounds derived from the asymptotics in the large argument regime ($\mathrm{R_i}$). The upper bound for $j'_{\nu,k}$ derived from the asymptotics in the transitional regime ($\mathrm{R_{ii}}$) from [EL97], [E01, §1.7] is listed in §4.

Unlike the previous approaches, we choose to work directly with the phase functions $\varphi_\nu(x)$ and $\theta_\nu(x)$ instead, using their non-oscillatory character and their known asymptotics in the Debye expansion region (R_{iii}). It has been known that these asymptotics give, in practice, good approximations of Bessel functions and their derivatives, and can be used for effective calculation of corresponding zeros with high precision, see [H017] as well as various generalisations in the important series of papers by Bremer, Rokhlin, et al. [HBRV15, HBR15, BR16, B17, B19]. Using techniques of Olver, Horsley [H017] has recently deduced asymptotics for the phase functions $\theta_\nu(x)$ and $\varphi_\nu(x)$ in the Debye region (R_{iii}). An extremely helpful feature of this problem is that, as it turns out, the expansions in the Debye region also give effective expansions in the large-argument region, and only weaken when one proceeds deep into the transition region. Further, it turns out that truncating these expansions leads to lower and upper bounds for phase functions: the error terms are sign-definite for a broad range of values. We prove this using a consequence of the Sturm comparison theorem (Theorem 2.5) combined with the non-oscillatory nature of the phase functions. The more detailed comparison of our bounds with existing ones and their effectiveness will be addressed in §4.

The rest of the paper is organised as follows. In §§1.4–1.7, we define the necessary auxiliary functions, study their properties, and state our main results, illustrating them graphically. All the proofs, together with additional Sturm–Liouville theory required, are collected in §2. In §3, we extend our techniques to obtain the bounds on the zeros of derivatives of *ultraspherical* Bessel functions. As we have mentioned, §4 discusses the comparison of our results with older ones, based on numerical evidence collected in Appendix B. In order not to overload the main text, some complicated intermediate expressions are placed in Appendix A.

We remark that many of the proofs involve straightforward but rather cumbersome manipulations with explicit functions. Although we have verified them independently by hand, we have relied in some cases on simplifications using `Mathematica`. In the interest of transparency, the corresponding script, as well as its printout, containing *all* of the analytic and numerical calculations we performed, including plotting routines, is available for inspection and download at

`https://michaellevitin.net/bessels.html`.

§1.4. Definitions and properties of the auxiliary functions I

We start by defining the following auxiliary functions. Everywhere below $x \geq \nu \geq 0$.

We define

$$\widetilde{\theta}_\nu(x) := \sqrt{x^2-\nu^2} - \nu \arccos\frac{\nu}{x} - \frac{\pi}{4},$$

and note that

$$\widetilde{\theta}_\nu(\nu) = -\frac{\pi}{4},$$

$$\widetilde{\theta}_\nu(x) = x - \frac{\pi}{4}(2\nu+1) + \frac{\nu^2}{2x} + O\left(x^{-3}\right) \qquad \text{as } x \to +\infty. \tag{1.9}$$

We also note that

$$\widetilde{\theta}'_\nu(x) = \frac{\sqrt{x^2-\nu^2}}{x} > 0 \qquad \text{for } x > \nu.$$

Therefore, the function $\widetilde{\theta}_\nu$ is strictly monotone increasing on the interval $(\nu, +\infty)$, and thus the inverse function

$$\left(\widetilde{\theta}_\nu\right)^{-1} : \left[-\frac{\pi}{4}, +\infty\right) \to [\nu, +\infty)$$

is well-defined.

Further, we set

$$\underline{\theta}_\nu(x) := \widetilde{\theta}_\nu(x) - \frac{3x^2+2\nu^2}{24(x^2-\nu^2)^{3/2}} = \sqrt{x^2-\nu^2} - \nu\arccos\frac{\nu}{x} - \frac{\pi}{4} - \frac{3x^2+2\nu^2}{24(x^2-\nu^2)^{3/2}},$$

and note that

$$\underset{\sim}{\theta}_\nu(x) \to -\infty \quad \text{as } x \to \nu^+,$$

$$\underset{\sim}{\theta}_\nu(x) = x - \frac{\pi}{4}(2\nu+1) + \frac{4\nu^2-1}{8x} + \frac{\nu^2\left(2\nu^2-13\right)}{48x^3} + O\left(x^{-5}\right) \qquad \text{as } x \to +\infty. \tag{1.10}$$

We also have

$$\underset{\sim}{\theta}_\nu'(x) = \frac{8x^6 + \left(1-24\nu^2\right)x^4 + 4\left(6\nu^4+\nu^2\right)x^2 - 8\nu^6}{8x(x^2-\nu^2)^{5/2}},$$

and therefore

$$\underset{\sim}{\theta}_\nu'\left(\sqrt{\nu^2+\chi}\right) = \frac{8\chi^3+\chi^2+6\chi\nu^2+5\nu^4}{8\chi^{5/2}\sqrt{\nu^2+\chi}} > 0 \qquad \text{for } \chi > 0.$$

Hence the function $\underset{\sim}{\theta}_\nu$ is strictly monotone increasing on the interval $(\nu, +\infty)$, and the inverse function

$$\left(\underset{\sim}{\theta}_\nu\right)^{-1} : \mathbb{R} \to (\nu, +\infty)$$

is well-defined.

Remark 1.3. We should explain the origin of the functions $\widetilde{\theta}_\nu(x)$ and $\underset{\sim}{\theta}_\nu(x)$: they represent, correspondingly, the two- and three-term asymptotic expansions of $\theta_\nu(x)$ in the Debye regime ($\mathrm{R_{iii}}$), see [Ho17, formula (34)], which are obtained using the algorithm of [O74]. ◀

§1.5. Main results I: bounding the phase and zeros of Bessel functions

Set, for $x > \nu \geq 0$,

$$\underset{\approx}{\theta}_\nu(x) := \max\left\{\underset{\sim}{\theta}_\nu(x), -\frac{\pi}{2}\right\}.$$

We have

Theorem 1.4. *For every $\nu \geq 0$ and every $x > \nu$,*

$$\underset{\approx}{\theta}_\nu(x) < \theta_\nu(x) < \widetilde{\theta}_\nu(x). \tag{1.11}$$

Remark 1.5. The upper bound in Theorem 1.4 has been already proved, using different techniques, in [S23] and [FLPS23]. ◀

Recalling (1.2) and (1.3), Theorem 1.4 immediately implies

Corollary 1.6. *For every $\nu \geq 0$, we have the following bounds.*

(i) *For every $k \in \mathbb{N}$,*

$$\underset{\sim}{j}_{\nu,k} := \left(\widetilde{\theta}_\nu\right)^{-1}\left(\pi\left(k-\frac{1}{2}\right)\right) < j_{\nu,k} < \left(\underset{\sim}{\theta}_\nu\right)^{-1}\left(\pi\left(k-\frac{1}{2}\right)\right) =: \widetilde{j}_{\nu,k}.$$

(ii) *For every $k \in \mathbb{N}$,*

$$\underset{\sim}{y}_{\nu,k} := \left(\widetilde{\theta}_\nu\right)^{-1}(\pi(k-1)) < y_{\nu,k} < \left(\underset{\sim}{\theta}_\nu\right)^{-1}(\pi\,(k-1)) =: \widetilde{y}_{\nu,k}.$$

(iii) *More generally, for all $\tau \in (0,1]$ and all $k \geq 2$, we have*

$$\underset{\sim}{c}_{\nu,\tau,k} := \left(\widetilde{\theta}_\nu\right)^{-1}\left(\pi\left(\tau+k-\frac{3}{2}\right)\right) < c_{\nu,\tau,k} < \left(\underset{\sim}{\theta}_\nu\right)^{-1}\left(\pi\left(\tau+k-\frac{3}{2}\right)\right) =: \widetilde{c}_{\nu,\tau,k}.$$

For $k = 1$, the upper bound $c_{\nu,\tau,1} < \widetilde{c}_{\nu,\tau,1}$ is also valid for all $\tau \in (0,1]$, and the lower bound $\underset{\sim}{c}_{\nu,\tau,1} < c_{\nu,\tau,1}$ is valid for $\tau \in \left(\frac{1}{4}, 1\right]$.

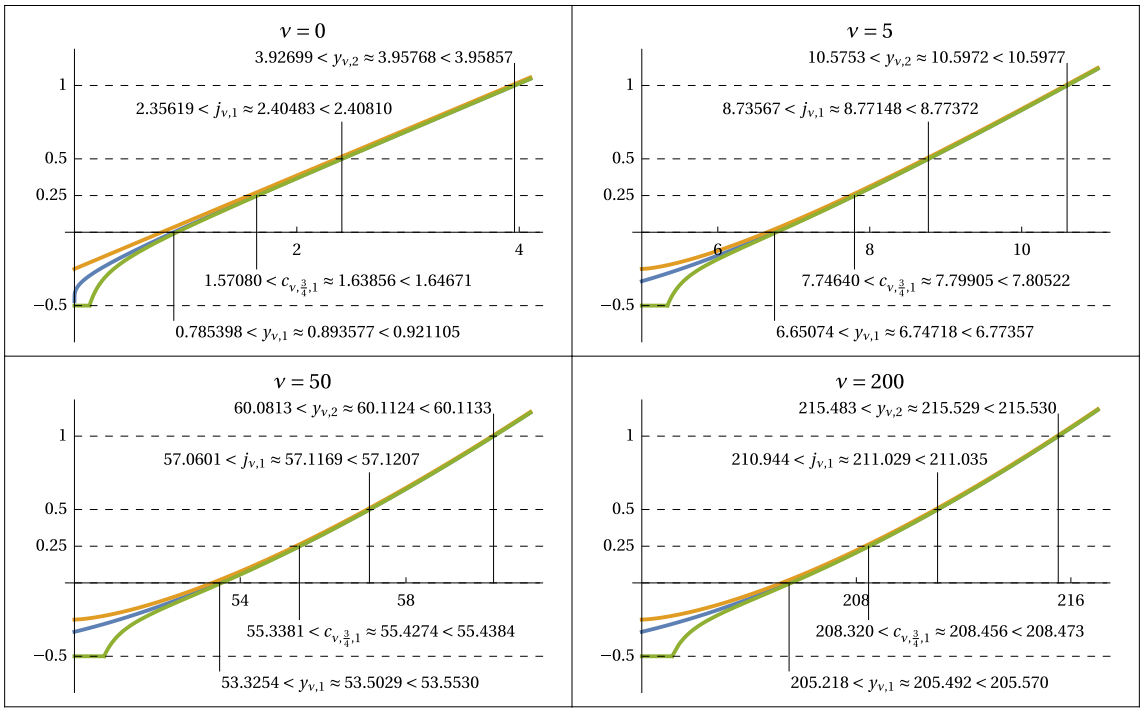

Figure 6: All plots show the scaled Bessel phase function $\frac{1}{\pi}\theta_\nu(x)$ (blue), and its scaled bounds $\frac{1}{\pi}\widetilde{\theta}_\nu(x)$ (orange) and $\frac{1}{\pi}\underset{\sim}{\theta}_\nu(x)$ (green). The zeros $c_{\nu,\frac{3}{4},1}$ are the first positive zeros of $\mathscr{C}_{\nu,\frac{3}{4}}(x)$, which up to a constant factor coincides with $J_\nu(x) - Y_\nu(x)$.

In part (iii), the restriction on the range of τ for which the lower bound holds with $k = 1$ is due to the necessary condition $\pi\left(\tau + \frac{1}{2}\right) > -\frac{\pi}{4}$ for applying the inverse function.

For an illustration of the results in Theorem 1.4 and Corollary 1.6, see Figure 6.

We also immediately deduce the bounds for the counting function (1.4) of Bessel zeros.

Corollary 1.7. *For any $\lambda > \nu \geq 0$,*

$$\left\lfloor \frac{1}{\pi}\underset{\sim}{\theta}_\nu(\lambda) + \frac{1}{2} \right\rfloor \leq \mathcal{N}_{J_\nu}(\lambda) \leq \left\lfloor \frac{1}{\pi}\widetilde{\theta}_\nu(\lambda) + \frac{1}{2} \right\rfloor,$$

where $\lfloor\cdot\rfloor$ denotes the integer part.

§1.6. Definitions and properties of the auxiliary functions II

We define, for $x > \nu \geq 0$, the functions

$$\underset{\sim}{\varphi}_\nu(x) := \widetilde{\theta}_\nu(x) + \frac{\pi}{2} = \sqrt{x^2 - \nu^2} - \nu \arccos\frac{\nu}{x} + \frac{\pi}{4}, \tag{1.12}$$

and

$$\widetilde{\varphi}_\nu(x) := \underset{\sim}{\varphi}_\nu(x) + \frac{9x^2 - 2\nu^2}{24(x^2-\nu^2)^{3/2}} = \sqrt{x^2 - \nu^2} - \nu \arccos\frac{\nu}{x} + \frac{\pi}{4} + \frac{9x^2 - 2\nu^2}{24(x^2-\nu^2)^{3/2}}.$$

As in §1.4, we have

$$\underset{\sim}{\varphi}_\nu(\nu) = \frac{\pi}{4},$$

$$\underset{\sim}{\varphi}_\nu(x) = x - \frac{\pi}{4}(2\nu-1) + \frac{\nu^2}{2x} + O\left(x^{-3}\right) \qquad \text{as } x \to +\infty. \tag{1.13}$$

Also,

$$\underset{\sim}{\varphi}'_\nu(x) = \widetilde{\theta}'_\nu(x) > 0 \qquad \text{for all } x > \nu \geq 0,$$

and the inverse function

$$\left(\underset{\sim}{\varphi}_\nu\right)^{-1} : \left[\frac{\pi}{4}, +\infty\right) \to [\nu, +\infty)$$

is well-defined. Moreover,

$$\left(\underset{\sim}{\varphi}_\nu\right)^{-1}(z) = \left(\widetilde{\theta}_\nu\right)^{-1}\left(z - \frac{\pi}{2}\right).$$

The behaviour of the function $\widetilde{\varphi}_\nu(x)$ is more complicated. We have

$$\widetilde{\varphi}_\nu(x) \to +\infty \quad \text{as } x \to \nu^+,$$

and

$$\widetilde{\varphi}_\nu(x) = x - \frac{\pi}{4}(2\nu-1) + \frac{4\nu^2+3}{8x} + \frac{\nu^2\left(2\nu^2+23\right)}{48x^3} + O\left(x^{-5}\right) \qquad \text{as } x \to +\infty. \tag{1.14}$$

Further,

$$\widetilde{\varphi}'_\nu(x) = \frac{p_\nu(x)}{8x\left(x^2-\nu^2\right)^{5/2}},$$

where

$$p_\nu(x) := 8x^6 - 3\left(8\nu^2+1\right)x^4 + 4\nu^2\left(6\nu^2-1\right)x^2 - 8\nu^6 \tag{1.15}$$

is not sign-definite for $x \in [\nu, +\infty)$. Namely, we will prove

Lemma 1.8. *For any $\nu \geq 0$, we have $\widetilde{\varphi}'_\nu(x) > 0$ for $x \in \left(x^\star_\nu, +\infty\right)$, where $x^\star_\nu$ is the only root in $(\nu, +\infty)$ of (1.15). The quantity*

$$z^\star_\nu := \widetilde{\varphi}_\nu\left(x^\star_\nu\right)$$

is positive and monotone decreasing in ν for all $\nu \geq 0$.

We present the graph of $\frac{1}{\pi}z^\star_\nu$ as a function of ν in Figure 7. Note that $x^\star_0 = \sqrt{\frac{3}{8}}$ and $z^\star_0 = \frac{\pi}{4} + \sqrt{\frac{3}{2}}$. It may be also shown that

$$x^\star_\nu = \nu + \frac{\sqrt[3]{7\nu}}{4} + O\left(\nu^{-1/3}\right), \qquad z^\star_\nu = \frac{\pi}{4} + \sqrt{\frac{7}{18}} + O\left(\nu^{-2/3}\right) \qquad \text{as } \nu \to +\infty.$$

Lemma 1.8 now ensures that the inverse function

$$\left(\underset{\sim}{\varphi}_\nu\right)^{-1} : \left[z^\star_\nu, +\infty\right) \to \left[x^\star_\nu, +\infty\right)$$

is well-defined.

Remark 1.9. Similarly to Remark 1.3, the functions $\underset{\sim}{\varphi}_\nu(x)$ and $\widetilde{\varphi}_\nu(x)$ represent, correspondingly, the two- and three-term asymptotic expansions of $\varphi_\nu(x)$ in the Debye regime ($\mathrm{R_{iii}}$), see [H017, formula (46)]. ◀

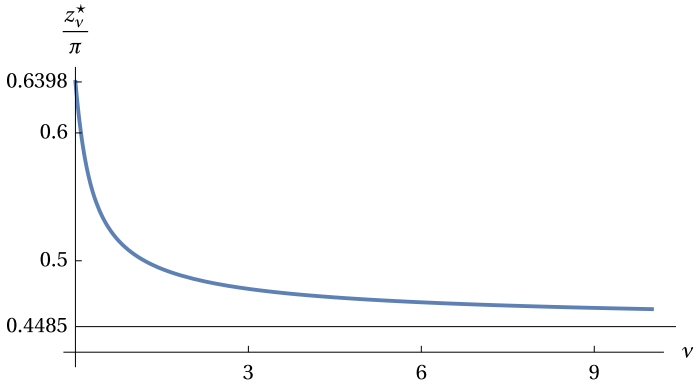

Figure 7: The plot of $\frac{1}{\pi} z_\nu^\star$ against ν, with the horizontal asymptote positioned at an approximate value of $\frac{1}{4} + \frac{1}{\pi}\sqrt{\frac{7}{18}}$.

§1.7. Main results II: bounding the phase and zeros of derivatives of Bessel functions

Set, for $x > \nu \geq 0$,

$$\widetilde{\widetilde{\varphi}}_\nu(x) := \begin{cases} z_\nu^\star & \text{if } x < x_\nu^\star, \\ \widetilde{\varphi}_\nu(x) & \text{if } x \geq x_\nu^\star. \end{cases}$$

Theorem 1.10. *For every $\nu \geq 0$ and every $x > \nu$, we have*

$$\underset{\sim}{\varphi}_\nu(x) < \varphi_\nu(x) < \widetilde{\widetilde{\varphi}}_\nu(x). \tag{1.16}$$

Remark 1.11. The lower bound in Theorem 1.10 has been already proved, using different techniques, in [FLPS23]. ◀

Recalling (1.6) and (1.7), Theorem 1.10 immediately implies

Corollary 1.12. *For every $\nu \geq 0$, we have the following bounds.*

(i) *For every $k \in \{2, 3, \dots\}$,*

$$\underset{\sim}{j}'_{\nu,k} := \left(\widetilde{\varphi}_\nu\right)^{-1}\left(\pi\left(k - \frac{1}{2}\right)\right) < j'_{\nu,k} < \left(\underset{\sim}{\varphi}_\nu\right)^{-1}\left(\pi\left(k - \frac{1}{2}\right)\right) =: \widetilde{j}'_{\nu,k}.$$

For $k = 1$, the upper bound $j'_{\nu,1} < \widetilde{j}'_{\nu,1}$ is also valid for all $\nu \geq 0$, and the lower bound $\underset{\sim}{j}'_{\nu,1} < j'_{\nu,1}$ is valid whenever

$$z_\nu^\star \leq \frac{\pi}{2},$$

that is, roughly, for $\nu \gtrsim 1.19876$.

(ii) *For every $k \in \mathbb{N}$,*

$$\underset{\sim}{y}'_{\nu,k} := \left(\widetilde{\varphi}_\nu\right)^{-1}(\pi k) < y'_{\nu,k} < \left(\underset{\sim}{\varphi}_\nu\right)^{-1}(\pi k) =: \widetilde{y}'_{\nu,k}.$$

(iii) *More generally, for all $\tau \in [0, 1)$ and all $k \geq 2$, we have*

$$\underset{\sim}{c}'_{\nu,\tau,k} := \left(\widetilde{\varphi}_\nu\right)^{-1}\left(\pi\left(\tau + k - \frac{1}{2}\right)\right) < c'_{\nu,\tau,k} < \left(\underset{\sim}{\varphi}_\nu\right)^{-1}\left(\pi\left(\tau + k - \frac{1}{2}\right)\right) =: \widetilde{c}'_{\nu,\tau,k}.$$

For $k = 1$, the upper bound $c'_{\nu,\tau,1} < \widetilde{c}'_{\nu,\tau,1}$ is also valid for all $\tau \in [0, 1)$. The lower bound $\underset{\sim}{c}'_{\nu,\tau,1} < c'_{\nu,\tau,1}$ is valid for ν such that

$$z_\nu^\star \leq \pi\left(\tau + \frac{1}{2}\right);$$

in particular, if $\tau \geq \frac{1}{\pi} z_0^\star - \frac{1}{2} = \frac{1}{\pi}\sqrt{\frac{3}{2}} - \frac{1}{4} \approx 0.139848$, then it is valid for all $\nu \geq 0$, see Figure 8.

In parts (i) and (iii), the restriction on the range of ν and τ for which the lower bound holds with $k = 1$ is due to the fact that the argument of the inverse function $\left(\widetilde{\varphi}_\nu\right)^{-1}$ should exceed $z_\nu^\star$.

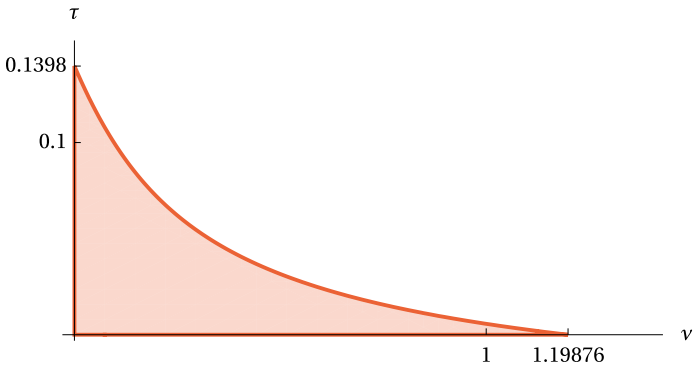

Figure 8: The region of the (ν, τ)-plane in which the lower bound $\underset{\sim}{c}'_{\nu,\tau,1} < c'_{\nu,\tau,1}$ for the first zero is *not applicable*.

For an illustration of the results in Theorem 1.10 and Corollary 1.12, see Figure 9.

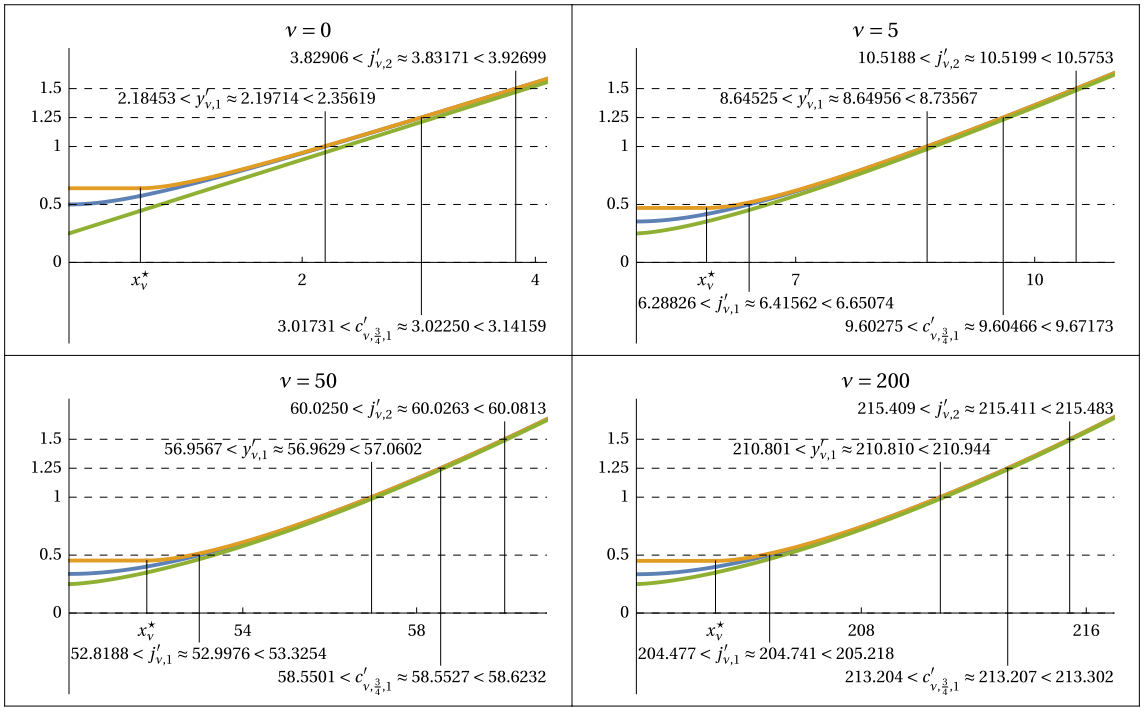

Figure 9: All plots show the scaled Bessel derivative phase function $\frac{1}{\pi}\varphi_\nu(x)$ (blue), and its scaled bounds $\frac{1}{\pi}\widetilde{\widetilde{\varphi}}_\nu(x)$ (orange) and $\underset{\sim}{\varphi}_\nu(x)$ (green). The zeros $c'_{\nu,\frac{3}{4},1}$ are the first zeros above $j'_{\nu,1}$ of $\mathscr{C}'_{\nu,\frac{3}{4}}(x)$, which up to a constant factor coincides with $J'_\nu(x) - Y'_\nu(x)$.

We also immediately deduce the bounds for the counting function (1.8) of zeros of Bessel derivatives.

Corollary 1.13. *For any* $\lambda > \nu \geq 0$,

$$\left\lfloor \frac{1}{\pi}\underset{\sim}{\varphi}_\nu(\lambda) + \frac{1}{2} \right\rfloor \leq \mathcal{N}_{J'_\nu}(\lambda) \leq \left\lfloor \frac{1}{\pi}\widetilde{\widetilde{\varphi}}_\nu(\lambda) + \frac{1}{2} \right\rfloor.$$

§2. Proofs

§2.1. Liouville's transformation and phase functions

Consider a real-valued function $f \in C^3(a,+\infty)$, $a \in \mathbb{R}$, with $f'(x) > 0$ for $x > a$. For $t \in \mathbb{R}$, we define the functions

$$\mathscr{F}_{f,t}(x) := \frac{\cos\big(f(x) - \pi t\big)}{\sqrt{f'(x)}}$$

and

$$\mathscr{V}_f(x) := \big(f'(x)\big)^2 + \frac{1}{2}\frac{f'''(x)}{f'(x)} - \frac{3}{4}\left(\frac{f''(x)}{f'(x)}\right)^2. \tag{2.1}$$

The following simple result is verified by a direct substitution, cf. [EL00, Lemma 1].

Lemma 2.1. *Under the above conditions, the function $\mathscr{F}_{f,t}(x)$ satisfies on $(a,+\infty)$ the Schrödinger equation*

$$\mathscr{F}''_{f,t}(x) + \mathscr{V}_f(x)\mathscr{F}_{f,t}(x) = 0. \tag{2.2}$$

Remark 2.2. The relation (2.1) is called *Liouville's transformation* in [H017] and *Kummer's equation* in [HBRV15, §1]. ◀

Let now $\mathscr{A}_1(x)$ and $\mathscr{A}_2(x)$ be two real linearly independent solutions of a Schrödinger equation

$$\mathscr{A}''(x) + \mathscr{P}(x)\mathscr{A}(x) = 0 \tag{2.3}$$

on $(a,+\infty)$, with a real-valued potential $\mathscr{P} \in C(a,+\infty)$. We define the modulus function $\mathscr{M}(x) = \mathscr{M}_{\mathscr{A}_1,\mathscr{A}_2}(x)$ and the phase function $\Psi(x) = \Psi_{\mathscr{A}_1,\mathscr{A}_2}(x)$ for these solutions as

$$\mathscr{M}(x) := \sqrt{(\mathscr{A}_1(x))^2 + (\mathscr{A}_2(x))^2}, \qquad \mathscr{A}_1(x) + \mathrm{i}\mathscr{A}_2(x) = \mathscr{M}(x)\exp\big(\mathrm{i}\Psi(x)\big),$$

where we choose a continuous branch of $\Psi(x) = \operatorname{Arctan}\frac{\mathscr{A}_2(x)}{\mathscr{A}_1(x)}$ specified by the chosen value of

$$\lim_{x\to a^+}\Psi(x).$$

Lemma 2.3. *We have*

$$\Psi'(x) = \frac{\mathscr{W}\{\mathscr{A}_1(x),\mathscr{A}_2(x)\}}{\mathscr{M}(x)^2},$$

where $\mathscr{W}\{\cdot,\cdot\}$ is the Wronskian of the two solutions, cf. [HBRV15, §1].

Assume additionally that $\Psi'(x) > 0$ for $x \in (a,+\infty)$. Then for any $t \in \mathbb{R}$, the function

$$\mathscr{A}(x) := \mathscr{F}_{\Psi,t}(x)$$

also satisfies (2.3)*, and therefore*

$$\mathscr{V}_\Psi(x) = \mathscr{P}(x).$$

Proof. The first statement is verified by direct differentiation:

$$\Psi'(x) = \frac{\mathrm{d}}{\mathrm{d}x}\arctan\frac{\mathscr{A}_2(x)}{\mathscr{A}_1(x)} = \frac{\mathscr{A}_1(x)\mathscr{A}_2'(x) - \mathscr{A}_2(x)\mathscr{A}_1'(x)}{(\mathscr{A}_1(x))^2 + (\mathscr{A}_2(x))^2}.$$

Since

$$\mathscr{F}_{\Psi,t}(x) = \frac{\cos(\pi t)\mathscr{A}_1(x) + \sin(\pi t)\mathscr{A}_2(x)}{\sqrt{\mathscr{W}}},$$

where $\mathscr{W} = \mathscr{W}\{\mathscr{A}_1(x),\mathscr{A}_2(x)\}$ is a constant which we assumed to be positive, the second statement also follows immediately once we have taken into account that $\mathscr{A}_1(x)$ and $\mathscr{A}_2(x)$ both satisfy (2.3). □

Lemma 2.3 implies

Lemma 2.4. *For the Bessel phase function $\theta_\nu(x)$, we have the Schrödinger equation (2.2), namely,*

$$\mathscr{F}''_{\theta_\nu,t}(x) + \mathscr{V}_{\theta_\nu}(x)\mathscr{F}_{\theta_\nu,t}(x) = 0$$

valid in the interval $(0,+\infty)$ for all $\nu \geq 0$ and $t \in \mathbb{R}$, with

$$\mathscr{V}_{\theta_\nu}(x) = 1 - \frac{\nu^2 - 1/4}{x^2}. \tag{2.4}$$

Similarly, for the Bessel derivative phase function $\varphi_\nu(x)$, we also have the Schrödinger equation (2.2), namely,

$$\mathscr{F}''_{\varphi_\nu,t}(x) + \mathscr{V}_{\varphi_\nu}(x)\mathscr{F}_{\varphi_\nu,t}(x) = 0$$

valid in the interval $(\nu,+\infty)$ for all $\nu \geq 0$ and $t \in \mathbb{R}$, with

$$\mathscr{V}_{\varphi_\nu}(x) = 1 - \frac{\nu^2 - \frac{1}{4}}{x^2} - \frac{2\nu^2 + x^2}{\left(x^2 - \nu^2\right)^2}. \tag{2.5}$$

Proof. We note that for all cylindrical functions $\mathscr{C}_{\nu,\tau}(x)$, and in particular for $J_\nu(x)$ and $Y_\nu(x)$, we have the Schrödinger equation

$$\left(\sqrt{x}\mathscr{C}_{\nu,\tau}(x)\right)'' + \left(1 - \frac{\nu^2 - 1/4}{x^2}\right)\left(\sqrt{x}\mathscr{C}_{\nu,\tau}(x)\right) = 0,$$

see [DLMF, (10.13.1)]; it can be easily checked directly. By Lemma 2.3, since $\theta_\nu(x) = \Psi_{\sqrt{x}J_\nu,\sqrt{x}Y_\nu}(x)$ has a positive derivative on $(\nu,+\infty)$, we conclude that $\mathscr{F}_{\varphi_\nu,t}$ satisfies the Schrödinger equation with the same potential, thus proving (2.4). We note that (2.4) can be found in [DLMF, (10.18.16)].

In the same manner, we have for $\mathscr{C}'_{\nu,\tau}(x)$, and in particular for $J'_\nu(x)$ and $Y'_\nu(x)$,

$$\left(\frac{x^{3/2}}{\sqrt{x^2-\nu^2}}\mathscr{C}'_{\nu,\tau}(x)\right)'' + \left(1 - \frac{\nu^2 - \frac{1}{4}}{x^2} - \frac{2\nu^2 + x^2}{\left(x^2 - \nu^2\right)^2}\right)\left(\frac{x^{3/2}}{\sqrt{x^2-\nu^2}}\mathscr{C}'_{\nu,\tau}(x)\right) = 0,$$

which is straightforward to verify directly or deduce from [DLMF, (10.13.7)], and the result follows from the observation that $\varphi_\nu(x) = \Psi_{\frac{x^{3/2}}{\sqrt{x^2-\nu^2}}J'_\nu,\frac{x^{3/2}}{\sqrt{x^2-\nu^2}}Y'_\nu}(x)$ has a positive derivative on $(\nu,+\infty)$. □

§2.2. A consequence of the Sturm comparison theorem

We state the following result which follows from the Sturm comparison theorem, and which will be used for comparing phase functions and their bounds. This is different from a common method of comparing zeros, cf. [He70] and [EL00].

Theorem 2.5. *Consider, for $a \in \mathbb{R}$, two functions $g, h \in C^3(a,+\infty)$ with positive derivatives and satisfying the following conditions:*

(C_1) $\lim_{x\to+\infty} g(x) = \lim_{x\to+\infty} h(x) = +\infty$;

(C_2) $\mathscr{V}_g(x) > \mathscr{V}_h(x)$ *for all* $x \in (a,+\infty)$;

(C_3) *there exists $b \geq a$ such that $g(x) < h(x)$ for all $x > b$.*

Then in fact $g(x) < h(x)$ for all $x > a$.

Remark 2.6. Our typical use of Theorem 2.5 can be illustrated by the following generic example.

Suppose that $g(x)$ is a phase function $\Psi_{\mathscr{A}_1,\mathscr{A}_2}(x)$ of two linearly independent solutions of the Schrödinger equation (2.3) with a given potential $\mathscr{P}(x)$, and $h(x)$ is some conjectured upper bound for $g(x)$. Assuming that both $g(x)$ and $h(x)$ have positive derivatives, we can use Lemma 2.3 to deduce that $\mathscr{V}_g(x) = \mathscr{P}(x)$, and therefore verification of (C_2) reduces to an explicit calculation.

In practice, we usually replace condition (C_3) by a stronger condition

(C_3') for some $s \in \mathbb{R}$, there exists the limit $\lim_{x\to+\infty} x^s\big(h(x)-g(x)\big)$, and it is positive.

This condition is easier to verify if the asymptotics of the phase function as $x \to +\infty$ is known. It is clear that (C_3') implies (C_3). ◀

Proof of Theorem 2.5. Suppose that the conclusion is wrong. Then there exists $x_0 > a$ for which $g(x_0) \geq h(x_0)$. Let $h_0 := h(x_0)$, $t_0 := \frac{1}{\pi}h_0 - \frac{1}{2}$, and consider the following two functions,

$$G(x) := \mathscr{F}_{g,t_0}(x) = \frac{\sin\big(g(x)-h_0\big)}{\sqrt{g'(x)}}, \qquad H(x) := \mathscr{F}_{h,t_0}(x) = \frac{\sin\big(h(x)-h_0\big)}{\sqrt{h'(x)}}.$$

Our assumptions imply that these function are both in $C^2(a,\infty)$, and, by Lemma 2.1, satisfy the differential equations

$$G''(x) + \mathscr{V}_g G(x) = 0, \qquad H''(x) + \mathscr{V}_h H(x) = 0$$

in that interval.

Due to condition (C_1), $H(x)$ has infinitely many zeros $\eta_k \in [x_0,\infty)$, one each time $h(\eta_k) - h_0 = \pi k$, for some sequence of consecutive $k \in \mathbb{Z}$. Note that $\eta_0 = x_0$, so that this sequence starts with $k = 0$. Similarly, $G(x)$ has a zero $\gamma_k \in [x_0,\infty)$ each time $g(\gamma_k) - h_0 = \pi k$ for another sequence of consecutive $k \in \mathbb{Z}$. Equivalently,

$$\gamma_k = g^{-1}(\pi k + h_0), \qquad \eta_k = h^{-1}(\pi k + h_0). \tag{2.6}$$

Observe that by our contradiction assumption, $g(x_0) - h_0 \geq 0$, or $\gamma_0 = g^{-1}(h_0) \leq x_0$, and so the first zero of $G(x)$ in (x_0,∞) is γ_m for some $m > 0$. By condition (C_2) and the Sturm comparison theorem, there exists at least one zero of $G(x)$ strictly between each pair of zeros of $H(x)$ on (x_0,∞). So, $G(x)$ has a zero in (η_0,η_1), and therefore we must have

$$\gamma_m < \eta_1 \leq \eta_m.$$

Similarly, there must be a zero of $G(x)$ in (η_m,η_{m+1}), and therefore $\gamma_{m+1} < \eta_{m+1}$. By induction, $\gamma_k < \eta_k$ for all $k \geq m$. However, by (2.6) and condition (C_3), we must have $\gamma_k > \eta_k$ for sufficiently large k. This contradiction completes the proof. □

§2.3. Proof of Theorem 1.4

We start with the upper bound. Applying Lemma 2.1 to $f := \widetilde{\theta}_\nu$ (which is defined and has a positive derivative on $(\nu,+\infty)$) with $t = 0$, we deduce that on this interval the function $\mathscr{F}_{\widetilde{\theta}_\nu,0}$ satisfies the Schrödinger equation

$$\mathscr{F}''_{\widetilde{\theta}_\nu,0}(x) + \mathscr{V}_{\widetilde{\theta}_\nu}(x)\mathscr{F}_{\widetilde{\theta}_\nu,0}(x) = 0,$$

with the potential

$$\mathscr{V}_{\widetilde{\theta}_\nu}(x) = \frac{4x^6 - 12\nu^2x^4 + 6\nu^2\left(2\nu^2-1\right)x^2 - \nu^4\left(4\nu^2-1\right)}{4x^2\left(x^2-\nu^2\right)^2}. \tag{2.7}$$

We want to apply Theorem 2.5 with

$$g(x) = \theta_\nu(x), \qquad h(x) = \widetilde{\theta}_\nu(x), \qquad a = \nu.$$

Condition (C_1) of Theorem 2.5 is obviously true. Verifying condition (C_2) is straightforward: we have, by (2.7) and (2.4),

$$\mathcal{V}_{\theta_\nu}(x) - \mathcal{V}_{\widetilde{\theta}_\nu}(x) = \frac{x^2+4\nu^2}{4(x^2-\nu^2)^2} > 0 \qquad \text{for all } x > \nu.$$

According to Remark 2.6, it remains to check condition (C_3'). The comparison of the asymptotics (1.1) and (1.9) yields

$$\widetilde{\theta}_\nu(x) - \theta_\nu(x) = \frac{1}{8x} + O\left(x^{-3}\right) \qquad \text{as } x \to +\infty,$$

and therefore (C_3') holds in this case with $s = 1$. Thus all conditions of Theorem 2.5 are fulfilled, which proves the upper bound in (1.11).

Instead of proving the lower bound in (1.11), we first establish a weaker bound

$$\underset{\sim}{\theta}_\nu(x) < \theta_\nu(x). \tag{2.8}$$

In order to prove (2.8) we act in the same manner as above, this time applying Theorem 2.5 with

$$g(x) = \underset{\sim}{\theta}_\nu(x), \qquad h(x) = \theta_\nu(x), \qquad a = \nu.$$

The expression for $\mathcal{V}_{\underset{\sim}{\theta}_\nu}(x)$ is given in Appendix A.

Condition (C_1) of Theorem 2.5 is obviously true, and verifying condition (C_2) requires the change of variable $x = \sqrt{\nu^2+\chi}$ with $\chi > 0$, which gives, by (2.4) and (A.1)–(A.3),

$$\begin{gathered}
64\chi^5\left(8\chi^3+\chi^2+6\nu^2\chi+5\nu^4\right)^2\left(\mathcal{V}_{\underset{\sim}{\theta}_\nu}\left(\sqrt{\nu^2+\chi^2}\right) - \mathcal{V}_{\theta_\nu}\left(\sqrt{\nu^2+\chi^2}\right)\right) = \\
1600\chi^9 + \left(33984\nu^2+16\right)\chi^8 + \left(99008\nu^4+784\nu^2+1\right)\chi^7 \\
+\left(70720\nu^4+1696\nu^2+23\right)\nu^2\chi^6 + 3\left(1376\nu^2+71\right)\nu^4\chi^5 + \left(5200\nu^2+1011\right)\nu^6\chi^4 \\
+5\left(400\nu^2+519\right)\nu^8\chi^3 + 3525\nu^{10}\chi^2 + 2375\nu^{12}\chi + 625\nu^{14}.
\end{gathered}$$

The right-hand side and the factor in the left-hand side are obviously positive for all $\chi > 0$, and thus $\mathcal{V}_{\underset{\sim}{\theta}_\nu}(x) > \mathcal{V}_{\theta_\nu}(x)$ for all $x > \nu$.

The validity of condition (C_3') follows from comparing (1.1) and (1.10), which gives

$$\theta_\nu(x) - \underset{\sim}{\theta}_\nu(x) = \frac{25}{384x^3} + O\left(x^{-4}\right) \qquad \text{as } x \to +\infty,$$

which implies (C_3') with $s = 3$. This shows that Theorem 2.5 is applicable and proves (2.8). The lower bound in (1.11) now follows as we know a priori that $\theta_\nu(x) > -\frac{\pi}{2}$ for all $x > \nu \geq 0$.

§2.4. Proof of Lemma 1.8

The only two non-trivial aspects are that the root $x_\nu^\star$ of the sextic polynomial (1.15) is greater than ν, and that $z_\nu^\star$ is monotone decreasing in ν.

To address the former, the substitution $x = \sqrt{\nu^2+\xi}$, $\xi \geq 0$, turns (1.15) into

$$p_\nu\left(\sqrt{\nu^2+\xi}\right) = 8\xi^3 - 3\xi^2 - 10\nu^2\xi - 7\nu^4.$$

It is then elementary to check that $p_\nu(\nu) \leq 0$, $p_\nu\left(\sqrt{\nu^2+\xi}\right)$ is negative near $\xi = 0^+$, positive as $\xi \to +\infty$, and $\frac{\mathrm{d}p_\nu\left(\sqrt{\nu^2+\xi}\right)}{\mathrm{d}\xi}$ vanishes at the only positive point $\xi = \frac{1}{8} + \frac{\sqrt{80\nu^2+3}}{8\sqrt{3}}$, which completes the proof.

To address the latter aspect, suppose for contradiction that $\frac{\mathrm{d}z_\nu^\star}{\mathrm{d}\nu}$ vanishes for some $\nu = \mu > 0$. We have

$$0 = \left.\frac{\mathrm{d}z_\nu^\star}{\mathrm{d}\nu}\right|_{\nu=\mu} = \left.\frac{\mathrm{d}\widetilde{\varphi}_\nu\left(x_\nu^\star\right)}{\mathrm{d}\nu}\right|_{\nu=\mu} = \left.\frac{\partial\widetilde{\varphi}_\nu(x)}{\partial\nu}\right|_{(\nu,x)=(\mu,x_\mu^\star)} + \widetilde{\varphi}'_\mu\left(x_\mu^\star\right)\left.\frac{\mathrm{d}x_\nu^\star}{\mathrm{d}\nu}\right|_{\nu=\mu}. \tag{2.9}$$

The last term in the right-hand side (in which $'$ denotes, as usual, the derivative with respect to the argument), vanishes by the definition of $x_\nu^\star$, and the equation reduces, after explicit evaluation of $\frac{\partial\widetilde{\varphi}_\nu(x)}{\partial\nu}$ and the substitution

$$x_\mu^\star = \kappa\mu \qquad \text{with } \kappa > 1, \tag{2.10}$$

to

$$\mu^2 = \frac{23\kappa^2 - 2}{24\left(\kappa^2-1\right)^{5/2}\operatorname{arcsec}\kappa}. \tag{2.11}$$

We now recall that by (1.15) we still require

$$p_\mu(x_\mu^\star) = 0;$$

substituting (2.10) and (2.11) into this gives, after some simplifications and using $\kappa > 1$, the equation

$$\frac{23\kappa^4 - 25\kappa^2 + 2}{3\kappa^2\sqrt{\kappa^2-1}\left(3\kappa^2+4\right)} - \operatorname{arcsec}\kappa = 0. \tag{2.12}$$

Denote the left-hand side of (2.12) by $K(\kappa)$. Then $\lim_{\kappa\to1^+} K(\kappa) = 0$ and

$$K'(\kappa) = -\frac{16\left(\kappa^2-1\right)^{3/2}\left(6\kappa^2+1\right)}{3\kappa^3\left(3\kappa^2+4\right)^2}$$

is strictly negative for $\kappa > 1$. Therefore (2.12) cannot have any solutions with $\kappa > 1$, and in turn (2.9) cannot hold for any $\mu > 0$. The contradiction completes the proof.

§2.5. Proof of Theorem 1.10

We act similarly to §2.3, starting with the lower bound in (1.16). Since, by (1.12), $\varphi_\nu(x)$ differs from $\widetilde{\theta}_\nu(x)$ only by a constant, Lemma 2.1 shows that on $(\nu, +\infty)$, the function $\mathscr{F}_{\underset{\sim}{\varphi}_\nu,0}$ satisfies the Schrödinger equation

$$\mathscr{F}''_{\underset{\sim}{\varphi}_\nu,0}(x) + \mathscr{V}_{\underset{\sim}{\varphi}_\nu}(x)\mathscr{F}_{\underset{\sim}{\varphi}_\nu,0}(x) = 0,$$

with the potential

$$\mathscr{V}_{\underset{\sim}{\varphi}_\nu}(x) = \mathscr{V}_{\widetilde{\theta}_\nu}(x), \tag{2.13}$$

see (2.7).

We want to apply Theorem 2.5 with

$$g(x) = \underset{\sim}{\varphi}_\nu(x), \qquad h(x) = \varphi_\nu(x), \qquad a = \nu.$$

By (2.5), (2.13), and (2.7),

$$\mathscr{V}_{\underset{\sim}{\varphi}_\nu}(x) - \mathscr{V}_{\varphi_\nu}(x) = \frac{4\nu^2 + 3x^2}{4\left(x^2-\nu^2\right)^2} > 0 \qquad \text{for all } x > \nu,$$

thus verifying condition (C_2) of Theorem 2.5. Further, by (1.5) and (1.13),

$$\varphi_\nu(x) - \underset{\sim}{\varphi}_\nu(x) = \frac{3}{8x} + O\left(x^{-2}\right) \qquad \text{as } x \to +\infty,$$

confirming that condition (C_3') holds with $s = 1$. Thus, Theorem 2.5 is applicable and yields the lower bound in (1.16).

Before proving the upper bound in (1.16) in full generality, we will prove it for sufficiently large x by showing that

$$\varphi_\nu(x) < \widetilde{\varphi}_\nu(x) \qquad \text{for } x > x_\nu^\star. \tag{2.14}$$

Once this is done, the full bound follows easily: firstly, since $\varphi_\nu'\left(x_\nu^\star\right) > 0 = \widetilde{\varphi}_\nu'\left(x_\nu^\star\right)$, the strict inequality also holds for $x = x_\nu^\star$; the rest follows since $\varphi_\nu(x) < \varphi_\nu\left(x_\nu^\star\right)$ and $\widetilde{\varphi}_\nu(x) > \widetilde{\varphi}_\nu\left(x_\nu^\star\right) = z_\nu^\star$ for $x \in \left(\nu, x_\nu^\star\right)$.

We will prove (2.14) by applying Theorem 2.5 with

$$g(x) = \varphi_\nu(x), \qquad h(x) = \widetilde{\varphi}_\nu(x), \qquad a = x_\nu^\star.$$

Since $\widetilde{\varphi}_\nu'(x) > 0$ for $x \in \left(x_\nu^\star, +\infty\right)$ by Lemma 1.8, we can apply Lemma 2.1 on this interval to deduce that the function $\mathscr{F}_{\widetilde{\varphi}_\nu,0}$ satisfies there the Schrödinger equation

$$\mathscr{F}_{\widetilde{\varphi}_\nu,0}''(x) + \mathcal{V}_{\widetilde{\varphi}_\nu}(x)\mathscr{F}_{\widetilde{\varphi}_\nu,0}(x) = 0,$$

where the potential $\mathcal{V}_{\widetilde{\varphi}_\nu}(x)$ is given by (A.4)–(A.6).

In order to verify condition (C_2), we set

$$\delta_\nu(x) := 4096x^2\left(x^2-\nu^2\right)^{10}\left(\widetilde{\varphi}_\nu'(x)\right)^2\left(\mathcal{V}_{\varphi_\nu}(x) - \mathcal{V}_{\widetilde{\varphi}_\nu}(x)\right).$$

Since the first three factors in the definition of $\delta_\nu(x)$ are positive for $x > x_\nu^\star$, it is enough to show that

$$\delta_\nu(x) > 0 \qquad \text{for all } x > x_\nu^\star \tag{2.15}$$

to ensure that (C_2) holds. Explicit computation gives

$$\begin{aligned}\delta_\nu(x) = \;& 4032x^{18} + 16\left(1208\nu^2+27\right)x^{16} - \left(158656\nu^4+2640\nu^2+81\right)x^{14}\\ &+ 16\nu^2\left(20272\nu^4+701\nu^2-27\right)x^{12} - 16\nu^4\left(12796\nu^4+1415\nu^2+54\right)x^{10}\\ &- 64\nu^6\left(2338\nu^4-337\nu^2+12\right)x^8 + 64\nu^8\left(4543\nu^4-164\nu^2-4\right)x^6\\ &- 3584\nu^{12}\left(41\nu^2-1\right)x^4 + 1024\nu^{14}\left(17\nu^2-1\right)x^2 + 4096\nu^{18},\end{aligned}$$

and we will verify (2.15) separately in two cases.

Case $\nu = 0$. Since $x_0^\star = \sqrt{\frac{3}{8}}$ and

$$x^{-14}\delta_0(x)\big|_{x=\sqrt{\frac{3}{8}+\xi}} = 72\left(56\xi^2+48\xi+9\right) > 0 \qquad \text{for } \xi > 0,$$

(2.15) follows.

Case $\nu > 0$. We introduce the new variable $\zeta > 0$ via $x = \nu(1+\zeta)$, and note that

$$\begin{aligned}\nu^{-14}\delta_\nu(x) = \;& 64\zeta^6(\zeta+2)^6\left(63\zeta^6+378\zeta^5+1625\zeta^4+3980\zeta^3+5681\zeta^2+4410\zeta+1463\right)\nu^4\\ &+ 16\zeta^3(\zeta+1)^2(\zeta+2)^3\\ &\quad\times\left(27\zeta^8+216\zeta^7+672\zeta^6+1008\zeta^5+998\zeta^4+1304\zeta^3+1672\zeta^2+1120\zeta+343\right)\nu^2\\ &- (\zeta+1)^6\left(3\zeta^2+6\zeta+7\right)^4,\end{aligned}$$

and, since the coefficient of the ν^2-term above is always positive,

$$\begin{aligned}\nu^{-14}\delta_\nu(x) \geq \;& 64\zeta^6(\zeta+2)^6\left(63\zeta^6+378\zeta^5+1625\zeta^4+3980\zeta^3+5681\zeta^2+4410\zeta+1463\right)\nu^4\\ &- (\zeta+1)^6\left(3\zeta^2+6\zeta+7\right)^4.\end{aligned} \tag{2.16}$$

On the other hand, we have

$$x > x_\nu^\star \iff \nu^{-4} p_\nu(\nu(1+\zeta)) > 0 \iff \nu^4 \geq \frac{(\zeta+1)^4(3\zeta(\zeta+2)+7)^2}{64\zeta^6(\zeta+2)^6}.$$

Taking this into account in (2.16), we deduce that for $x > x_\nu^\star$,

$$\nu^{-14}\delta_\nu(x) \geq 2(\zeta+1)^4(3\zeta(\zeta+2)+7)^2(\zeta(\zeta+2)(\zeta(\zeta+2)(27\zeta(\zeta+2)+409)+1057)+707) > 0,$$

proving (2.15) in this case as well.

To finish the proof of (2.14) using Theorem 2.5, it remains to check condition (C_3'), for which we use (1.5) and (1.14) to deduce

$$\widetilde{\varphi}_\nu(x) - \varphi_\nu(x) = \frac{21}{128x^3} + O\big(x^{-4}\big) \qquad \text{as } x \to +\infty,$$

confirming that condition (C_3') holds with $s = 3$.

§3. Derivatives of ultraspherical Bessel functions

§3.1. Setup III

Let $\nu \geq 0$, $\eta \in \mathbb{R}$, and let

$$U_{\nu,\eta}(x) := x^{-\eta} J_\nu(x), \qquad W_{\nu,\eta}(x) := x^{-\eta} Y_\nu(x)$$

denote the *ultraspherical Bessel functions*. We will be interested in their derivatives

$$U'_{\nu,\eta}(x) = x^{-\eta-1}\big(xJ'_\nu(x) - \eta J_\nu(x)\big), \qquad W'_{\nu,\eta}(x) = x^{-\eta-1}\big(xY'_\nu(x) - \eta Y_\nu(x)\big),$$

in practise usually omitting the factor $x^{-\eta-1}$, see Figure 10, and denote by

$$u'_{\nu,\eta,k} \qquad \text{and} \qquad w'_{\nu,\eta,k}$$

the kth positive zero of $U'_{\nu,\eta}(x)$ and $W'_{\nu,\eta}(x)$, respectively, with the exception in case $\eta = \nu$,

$$u'_{\nu,\nu,1} := 0.$$

Of course, for $\eta = 0$ we return to the usual derivatives of Bessel functions and their zeros.

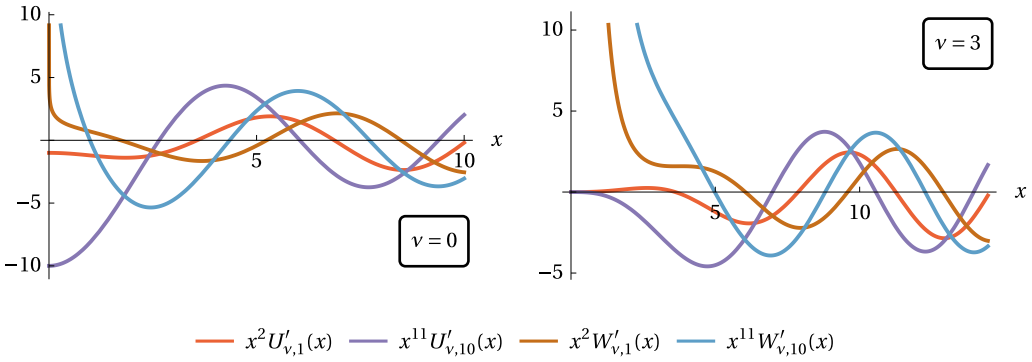

Figure 10: Plots of $x^{\eta+1}U'_{\nu,\eta}(x)$ and $x^{\eta+1}W'_{\nu,\eta}(x)$.

The function $U'_{\nu,\eta}(x)$ and, specifically, its zeros $u'_{\nu,\eta,k}$, play an important role in spectral geometry. In particular, for $d \geq 3$, the numbers

$$\left(u'_{m+\frac{d}{2}-1,\frac{d}{2}-1,k}\right)^2, \qquad m \in \mathbb{N} \cup \{0\},$$

are the eigenvalues of multiplicity

$$\binom{m+d-1}{d-1} - \binom{m+d-3}{d-1}$$

of the Neumann Laplacian on the unit ball in $\mathbb{R}^d$, see [AB93] and [LMP23, §1.2.3]. Also,

$$\left(u'_{m,\eta,k}\right)^2, \qquad m \in \mathbb{N} \cup \{0\},$$

are the non-negative eigenvalues of the Robin Laplacian in the unit disk in $\mathbb{R}^2$ with the Robin parameter $-\eta$, which are taken with multiplicity one if $m = 0$, and multiplicity two otherwise, see [BFK16].

For further properties of the derivatives of the ultraspherical Bessel functions and of their roots, including some bounds, see, e.g., [IS88], [LS94], and [L99]. In turn, we are primarily interested in the corresponding phase function which we define and discuss in the next section.

§3.2. Phase function of ultraspherical Bessel derivatives

As for the standard Bessel functions and their derivatives, we introduce the *modulus* and *phase functions* of the ultrasperical Bessel derivatives, $L_{\nu,\eta}, \psi_{\nu,\eta} : (0, +\infty) \to \mathbb{R}$ defined by

$$L_{\nu,\eta}(x) = \sqrt{\left(U'_{\nu,\eta}(x)\right)^2 + \left(W'_{\nu,\eta}(x)\right)^2}, \qquad U'_{\nu,\eta}(x) + \mathrm{i}W'_{\nu,\eta}(x) = L_{\nu,\eta}(x)\left(\cos\psi_{\nu,\eta}(x) + \mathrm{i}\sin\psi_{\nu,\eta}(x)\right),$$

where we choose a continuous branch of $\psi_{\nu,\eta}(x)$ with the initial condition

$$\lim_{x\to 0^+} \psi_{\nu,\eta}(x) = \frac{\pi}{2}.$$

Set, for $\nu \geq 0$, [1]

$$\mu^2_{\nu,\eta} = \mu^2 := \nu^2 - \eta^2,$$

and

$$I_{\nu,\eta} := \begin{cases} \left(\mu_{\nu,\eta}, +\infty\right) & \text{if } |\eta| < \nu, \\ (0, +\infty) & \text{if } |\eta| \geq \nu. \end{cases}$$

We have

Lemma 3.1. *Let $\nu \geq 0$, $\eta \in \mathbb{R}$, $x > 0$. If $\mu^2_{\nu,\eta} > 0$, then the function $\psi'_{\nu,\eta}(x)$ has a single zero at $x = \mu_{\nu,\eta}$ and is positive for $x > \mu_{\nu,\eta}$, otherwise its derivative is positive on the positive real line. Moreover, on the interval $I_{\nu,\eta}$, the function $\mathscr{F}_{\psi_{\nu,\eta},0}(x)$ satisfies the Schrödinger equation (2.2) with the potential*

$$\mathscr{V}_{\psi_{\nu,\eta}}(x) = 1 - \frac{\nu^2 - \frac{1}{4}}{x^2} + \frac{2(1-\eta)}{x^2 - \mu^2_{\nu,\eta}} - \frac{3x^2}{\left(x^2 - \mu^2_{\nu,\eta}\right)^2}.$$

[1] This is a convenient notation as we will not need to consider $\mu_{\nu,\eta}$ when $\mu^2_{\nu,\eta}$ is negative.

Proof. A direct differentiation shows that

$$\psi'_{\nu,\eta}(x) = \left(\arctan\frac{W'_{\nu,\eta}(x)}{U'_{\nu,\eta}(x)}\right)' = \frac{2\left(x^2-\mu^2_{\nu,\eta}\right)}{\pi x^{2\eta+3}L^2_{\nu,\eta}(x)}, \tag{3.1}$$

and the first statement then follows immediately since $L_{\nu,\eta}(x)$ does not vanish.

Set, for $x \in I_{\nu,\eta}$,

$$\mathscr{A}_1(x) := \frac{x^{\eta+3/2}}{\sqrt{x^2-\mu^2_{\nu,\eta}}}U'_{\nu,\eta}(x), \qquad \mathscr{A}_2(x) := \frac{x^{\eta+3/2}}{\sqrt{x^2-\mu^2_{\nu,\eta}}}W'_{\nu,\eta}(x).$$

A straightforward check shows that we have

$$\mathscr{A}''_j(x) + \left(1 - \frac{\nu^2-\frac14}{x^2} + \frac{2(1-\eta)}{x^2-\mu^2_{\nu,\eta}} - \frac{3x^2}{\left(x^2-\mu^2_{\nu,\eta}\right)^2}\right)\mathscr{A}_j(x) = 0, \qquad j=1,2,$$

and the second statement is obtained by Lemma 2.1. □

Lemma 3.1 ensures that the inverse function $\left(\psi_{\nu,\eta}\right)^{-1}$ is well-defined on $\left[\psi_{\nu,\eta}\left(\mu_{\nu,\eta}\right),+\infty\right)$ if $|\eta|<\nu$, or on $[0,+\infty)$ otherwise, and

$$u'_{\nu,\eta,k} = \left(\psi_{\nu,\eta}\right)^{-1}\left(\pi\left(k-\frac12\right)\right), \qquad w'_{\nu,\eta,k} = \left(\psi_{\nu,\eta}\right)^{-1}(\pi k). \tag{3.2}$$

We can establish the asymptotics of $\psi_{\nu,\eta}(x)$ for large x.

Lemma 3.2. *We have*

$$\begin{aligned}\psi_{\nu,\eta}(x) = x - \frac{\pi}{4}(2\nu-1) + \frac{4\nu^2+3+8\eta}{8x}\\ + \frac{16\nu^4+(192\eta+184)\nu^2-63-128\eta^3-192\eta^2-144\eta}{384x^3} + O\left(x^{-5}\right) \qquad \text{as } x\to+\infty.\end{aligned} \tag{3.3}$$

Proof. In essence, we emulate the approach of [HBRV15, §2] to the asymptotics of the standard Bessel phase function. Using standard asymptotics of the Bessel functions and their derivatives [DLMF, §10.17], we get first

$$x^{2\eta}L^2_{\nu,\eta}(x) = \frac{2}{\pi x} + \frac{8\eta^2+8\eta-4\nu^2+3}{4\pi x^3} + \frac{\left(4\nu^2-1\right)\left(16\eta^2+48\eta-4\nu^2+45\right)}{64\pi x^5} + O\left(x^{-7}\right) \qquad \text{as } x\to+\infty.$$

Computing the reciprocal of this series, substituting it into the right-hand side of the differential equation (3.1), and integrating term by term gives (3.3) except for the $O(1)$-term which, at this stage, is an unknown constant of integration C. Then, in the leading terms,

$$U'_{\nu,\eta}(x) = L_{\nu,\eta}(x)\cos\psi_{\nu,\eta}(x) \sim \sqrt{\frac{2}{\pi}}x^{-\eta-\frac12}\cos(x+C),$$

which should match the standard asymptotics

$$U'_{\nu,\eta}(x) \sim \sqrt{\frac{2}{\pi}}x^{-\eta-\frac12}\cos\left(x-\frac{\pi}{4}(2\nu-1)\right),$$

giving

$$C = -\frac{\pi}{4}(2\nu-1).$$

□

We are going to demonstrate that the uniform bounds on $\psi_{\nu,\eta}(x)$ can be obtained in the same manner as we have done for $\theta_\nu(x)$ and $\varphi_\nu(x)$, subject to some restrictions on x. Generally speaking, such bounds depend upon the signs of η and of $\mu^2_{\nu,\eta}$, so for brevity we from now on restrict ourselves to the case

$$\nu > \eta > 0 \tag{3.4}$$

(which implies $\mu^2_{\nu,\eta} > 0$) and to the lower bound on $\psi_{\nu,\eta}(x)$. See also Remark 3.7 for the case $\nu = \eta > 0$.

§3.3. Definitions and properties of the auxiliary functions III

Assuming (3.4), we from now on use the shorthand μ for $\mu_{\nu,\eta} = \sqrt{\nu^2 - \eta^2}$. We will keep using indices $\{\nu, \eta\}$ for some quantities but $\{\mu, \eta\}$ for some others where it simplifies the presentation, keeping the relation above in mind.

We define, for $x > \mu$, the function

$$\underset{\sim}{\psi}_{\nu,\eta}(x) := \sqrt{x^2 - \mu^2} - \left(\frac{\eta^2}{2\mu} + \mu\right) \arccos\frac{\mu}{x} + \frac{\eta}{\sqrt{x^2 - \mu^2}} + \frac{\pi}{4}\left(\frac{\eta^2}{\mu} + 2(\mu - \nu) + 1\right). \tag{3.5}$$

Remark 3.3. Similarly to Remarks 1.3 and 1.9, the function $\underset{\sim}{\psi}_{\nu,\eta}(x)$ coincides with the two-term asymptotic expansions of $\psi_{\nu,\eta}(x)$ in the Debye regime ($\mathrm{R_{iii}}$) deduced using the methods of [O74]. ◀

It is obvious that

$$\lim_{x\to\mu^+} \underset{\sim}{\psi}_{\nu,\eta}(x) = \lim_{x\to+\infty} \underset{\sim}{\psi}_{\nu,\eta}(x) = +\infty,$$

and easily checked that

$$\underset{\sim}{\psi}_{\nu,\eta}(x) = x - \frac{\pi}{4}(2\nu - 1) + \frac{\nu^2 + 2\eta}{2x} + O\left(x^{-3}\right) \qquad \text{as } x \to +\infty. \tag{3.6}$$

Further, it is easy to check that its derivative

$$\underset{\sim}{\psi}'_{\nu,\eta}(x) = \frac{2x^4 - x^2\left(\eta(\eta+2) + 4\mu^2\right) + \mu^2\left(\eta^2 + 2\mu^2\right)}{2x(x^2 - \mu^2)^{3/2}}$$

vanishes at the point

$$x^{\#}_{\mu,\eta} := \frac{1}{2}\sqrt{4\mu^2 + \eta(\eta+2) + \sqrt{\eta^2(\eta+2)^2 + 16\mu^2\eta}} > \mu,$$

and is positive for $x > x^{\#}_{\mu,\eta}$.

Therefore, the inverse function $\left(\underset{\sim}{\psi}_{\nu,\eta}\right)^{-1} : \left(\underset{\sim}{\psi}_{\nu,\eta}\left(x^{\#}_{\mu,\eta}\right), +\infty\right) \to \left(x_{\mu,\eta}, +\infty\right)$ is well-defined.

Set additionally, for $\mu \geq 0$, $\eta > 0$,

$$\begin{aligned}
r_{\mu,\eta}(x) := \;& 12x^{14} \\
&+ x^{12}\left(-44\mu^2 + 4\eta\left(\eta^3 + 4\eta^2 - 5\eta - 18\right)\right) \\
&+ x^{10}\left(40\mu^4 + 8\left(-3\eta^3 - 10\eta^2 + 6\eta + 5\right)\eta\mu^2 - \eta^2(\eta+2)^2\left(4\eta^2 + 8\eta - 3\right)\right) \\
&+ x^8\left(40\mu^6 + 4\left(15\eta^3 + 40\eta^2 + 2\eta + 70\right)\eta\mu^4\right. \\
&\qquad \left. + \left(20\eta^4 + 96\eta^3 + 147\eta^2 + 96\eta + 52\right)\eta^2\mu^2 + (\eta+2)^4\eta^4\right) \\
&+ x^6\left(-100\mu^8 - 8\eta\left(10\eta^3 + 20\eta^2 + 14\eta + 45\right)\mu^6\right. \\
&\qquad \left. - \eta^2\left(40\eta^4 + 144\eta^3 + 171\eta^2 + 116\eta + 80\right)\mu^4 - 4\eta^5(\eta+2)^3\mu^2\right) \\
&+ x^4\left(68\mu^{10} + 4\left(15\eta^3 + 20\eta^2 + 27\eta + 20\right)\eta\mu^8\right. \\
&\qquad \left. + \left(40\eta^4 + 96\eta^3 + 81\eta^2 + 24\eta + 16\right)\eta^2\mu^6 + 6(\eta+2)^2\eta^6\mu^4\right) \\
&+ x^2\left(-16\mu^{12} - 8\eta\left(3\eta^3 + 2\eta^2 + 4\eta - 4\right)\mu^{10} - 4\eta^3\left(5\eta^3 + 6\eta^2 + 3\eta - 4\right)\mu^8 - 4\eta^7(\eta+2)\mu^6\right) \\
&+ \left(4\eta^4\mu^{12} + 4\eta^6\mu^{10} + \eta^8\mu^8\right),
\end{aligned} \tag{3.7}$$

and let $x^{@}_{\mu,\eta}$ be the greatest positive real root of (3.7). It exists due to

Lemma 3.4. *For any $\mu \geq 0$, $\eta > 0$,*

$$x^{@}_{\mu,\eta} > x^{\#}_{\mu,\eta}.$$

Proof. Since the polynomial (3.7) has a positive leading term $12x^{14}$, it is sufficient to show that $r_{\mu,\eta}\left(x^{\#}_{\mu,\eta}\right) < 0$. With the shorthand $\rho := \sqrt{\eta^2(\eta+2)^2 + 16\mu^2\eta} > 0$, we get

$$\begin{aligned} r_{\mu,\eta}\left(x^{\#}_{\mu,\eta}\right) = &-\frac{3}{16}\eta^2\left(\eta(\eta+2)^2+16\mu^2\right) \\ &\times\left(\eta^9+10\eta^8+\eta^7\left(4\mu^2+\rho+40\right)+4\eta^6\left(13\mu^2+2\rho+20\right)+4\eta^5\left(\mu^4+\mu^2(\rho+54)+6\rho+20\right)\right. \\ &+4\eta^4\left(22\mu^4+\mu^2(9\rho+92)+8(\rho+1)\right)+4\eta^3\left(\mu^4(\rho+96)+8\mu^2(3\rho+7)+4\rho\right) \\ &\left.+16\eta^2\left(3\mu^6+\mu^4(3\rho+28)+5\mu^2\rho\right)+32\eta\left(7\mu^6+3\mu^4\rho\right)+16\mu^6\rho\right) < 0 \end{aligned}$$

as required. □

§3.4. Main results III: bounding the phase and zeros of derivatives of ultraspherical Bessel functions

Theorem 3.5. *For every $\nu > \eta > 0$ and every $x > x^{@}_{\mu,\eta}$, with $\mu = \mu_{\nu,\eta}$, we have*

$$\underset{\sim}{\psi}_{\nu,\eta}(x) < \psi_{\nu,\eta}(x).$$

Recalling (3.2), we deduce

Corollary 3.6. *For $\nu > \eta > 0$, we have the following bounds, valid for all $k \in \mathbb{N}$ such that the argument of the inverse function exceeds $\underset{\sim}{\psi}_{\nu,\eta}\left(x^{@}_{\mu,\eta}\right)$.*

(i)
$$u'_{\nu,\eta,k} < \left(\underset{\sim}{\psi}_{\nu}\right)^{-1}\left(\pi\left(k-\frac{1}{2}\right)\right).$$

(ii)
$$w'_{\nu,\eta,k} < \left(\underset{\sim}{\psi}_{\nu}\right)^{-1}(\pi k).$$

Remark 3.7. Formally, Theorem 3.5 and Corollary 3.6 are inapplicable when $\eta = \nu$, and therefore $\mu = 0$, since in that case the definition (3.5) does not make sense. If, however, we set, for $\nu > 0$ and $x > 0$,

$$\underset{\sim}{\psi}_{\nu,\nu}(x) := \lim_{\eta\to\nu^-}\underset{\sim}{\psi}_{\nu,\eta}(x) = x - \frac{\pi}{4}(2\nu-1) + \frac{\nu(\nu+2)}{2x},$$

both results become valid for $\eta = \nu$ without further modifications. ◀

For an illustration of the results in Theorem 3.5, Corollary 3.6, and Remark 3.7, see Figure 11.

Proof of Theorem 3.5. We will prove (2.14) by applying Theorem 2.5 with

$$g(x) = \underset{\sim}{\psi}_{\nu,\eta}(x), \qquad h(x) = \psi_{\nu,\eta}(x), \qquad a = x^{@}_{\mu,\eta}.$$

Both functions g and h have positive derivatives on $(a, +\infty)$ by Lemma 3.1 and analysis at the beginning of §3.3 (since $x^{@}_{\mu,\eta} > x^{\#}_{\mu,\eta} > \mu$) and tend to infinity at infinity. We can apply Lemma 2.1 on this interval to deduce that the function $\mathscr{F}_{\underset{\sim}{\psi}_{\nu,\eta},0}$ satisfies there the Schrödinger equation

$$\mathscr{F}''_{\underset{\sim}{\psi}_{\nu,\eta},0}(x) + \mathscr{V}_{\underset{\sim}{\psi}_{\nu,\eta}}(x)\mathscr{F}_{\underset{\sim}{\psi}_{\nu,\eta},0}(x) = 0,$$

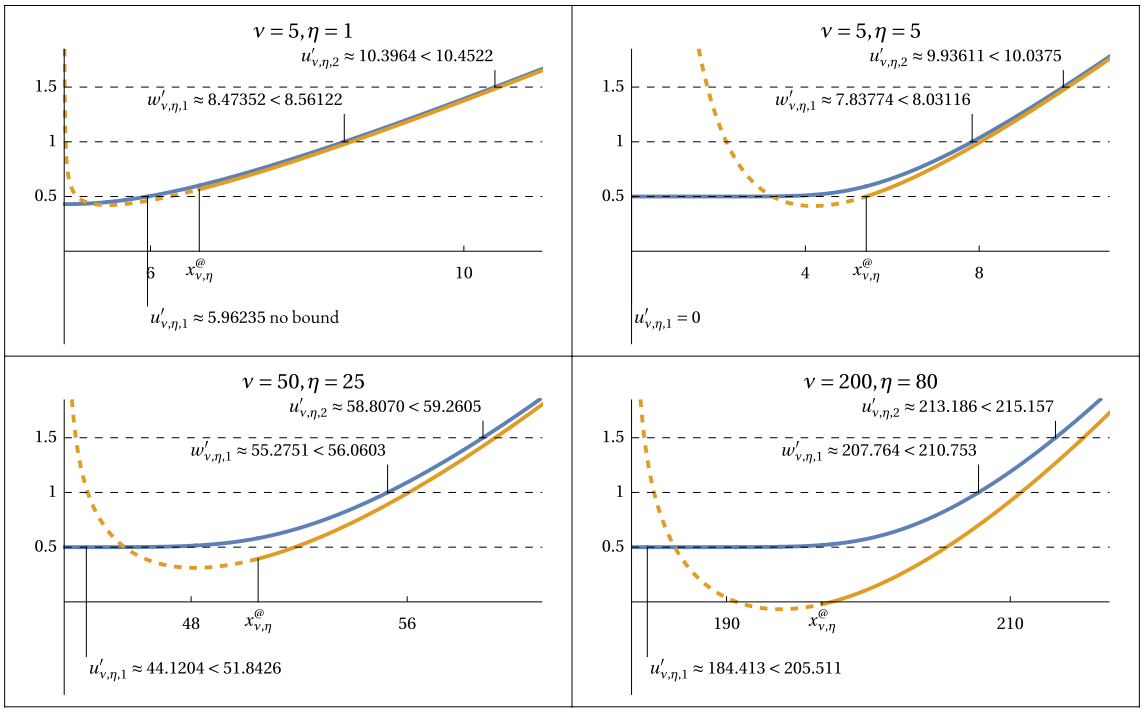

Figure 11: All plots show the scaled phase function $\frac{1}{\pi}\psi_\nu(x)$ (blue), and its scaled bound $\frac{1}{\pi}\underset{\sim}{\psi}_\nu(x)$ (orange). The quality of the bounds for $u'_{\nu,\eta,k}$ and $w'_{\nu,\eta,k}$ increases with k.

with the potential $\mathcal{V}_{\underset{\sim}{\psi}_{\nu,\eta}}(x)$ given by (A.7)–(A.9).

An explicit calculation yields

$$16x^4(x^2-\mu^2)^6\left(\underset{\sim}{\psi}'_{\nu,\eta}(x)\right)^2\left(\mathcal{V}_{\underset{\sim}{\psi}_{\nu,\eta}}(x)-\mathcal{V}_{\psi_{\nu,\eta}}(x)\right)=r_{\mu,\eta}(x),$$

where the right-hand side is given by (3.7). Since $r_{\mu,\eta}(x)>0$ for $x>a$, we have verified condition (C_2) of Theorem 2.5.

Condition (C'_3) holds with $s=1$ since by (3.3) and (3.6),

$$\psi_{\nu,\eta}(x)-\underset{\sim}{\psi}_{\nu,\eta}(x)=\frac{3}{8x}+O\left(x^{-3}\right)\qquad \text{as } x\to+\infty.$$

□

§4. Benchmarking and conclusions

In oder to set up comparison with previous bounds, we denote

$$A_\nu^{(1)}(\beta) := \beta,$$
$$A_\nu^{(2)}(\beta) := \beta - \frac{4\nu^2-1}{8\beta},$$
$$A_\nu^{(3)}(\beta) := \beta - \frac{4\nu^2-1}{8\beta} - \frac{4(4\nu^2-1)(28\nu^2-31)}{3(8\beta)^3}.$$

and let

$$\beta_{\nu,k} := \pi\left(k + \frac{\nu}{2} - \frac{1}{4}\right).$$

The i-term McMahon asymptotic expansion for the large zeros of the Bessel function of a *fixed* order $\nu \geq 0$, is given, for $i = 1,2,3$, by the formula

$$j_{\nu,k} = A_\nu^{(i)}\left(\beta_{\nu,k}\right) + O\left(\beta_{\nu,k}^{-2i+1}\right) \qquad \text{as } k \to +\infty, \tag{4.1}$$

see [M94], [W95, §15.53], [DLMF, (10.21.19)], and also [N21, Appendix A] for further terms. The remainder term may be alternatively written as $O\left(k^{-2(i-1)}\right)$. The more general asymptotic formulae for $c_{\nu,\tau,k}$ are obtained in the same manner by replacing $\beta_{\nu,k}$ with $\pi\left(k + \frac{\nu}{2} + \tau - \frac{5}{4}\right)$.

We have Hethcote's upper bound [He70]:

$$j_{\nu,k} \leq \begin{cases} A_\nu^{(2)}(\beta_{\nu,k}) & \text{if } \nu \leq \frac{1}{2}, \\ A_\nu^{(1)}(\beta_{\nu,k}) & \text{if } \nu > \frac{1}{2}, \end{cases} =: \widetilde{h}_{\nu,k} \qquad \text{for all } \nu \geq 0 \text{ and } k \in \mathbb{N}.$$

In the same paper, Hethcote also proves the lower bound (but only valid for small ν),

$$j_{\nu,k} \geq H_\nu^{(1)}(\beta_{\nu,k}) =: \underset{\sim}{h}_{\nu,k} \qquad \text{for all } 0 \leq \nu \leq \frac{1}{2} \text{ and } k \in \mathbb{N}.$$

Some improvements of Hethcote's bounds were obtained in [EL00]. Namely, they proved the upper bound

$$j_{\nu,k} \leq \begin{cases} A_\nu^{(2)}(\beta_{\nu,k}) & \text{if } \nu \leq \frac{1}{2}, \\ A_\nu^{(3)}(\beta_{\nu,k}) & \text{if } \nu > \frac{1}{2}, \end{cases} =: \widetilde{\ell}_{\nu,k} \qquad \text{for all } \nu \geq 0 \text{ and } k \in \mathbb{N}.$$

and the lower bound (for a slightly wider range of νs)

$$j_{\nu,k} \geq \begin{cases} A_\nu^{(3)}(\beta_{\nu,k}) & \text{if } \nu \leq \frac{1}{2}, \\ A_\nu^{(2)}(\beta_{\nu,k}) & \text{if } \frac{1}{2} < \nu < \sqrt{\frac{31}{28}}, \end{cases} =: \underset{\sim}{\ell}_{\nu,k} \qquad \text{for all } 0 \leq \nu < \sqrt{\frac{31}{28}} \text{ and } k \in \mathbb{N}.$$

For further improvements of these bounds when $\nu \leq \frac{1}{2}$, see [N21].

We note that we always have (when the bounds exist)

$$\underset{\sim}{h}_{\nu,k} \leq \underset{\sim}{\ell}_{\nu,k} < j_{\nu,k} < \widetilde{\ell}_{\nu,k} \leq \widetilde{h}_{\nu,k}. \tag{4.2}$$

Alternative bounds, based on the asymptotics of $j_{\nu,k}$ in the regime ($\mathrm{R_{ii}}$), were given by Qu and Wong [QW96]. Let

$$(0 >) a_1 > a_2 > \dots$$

denote the sequence of negative zeros of the Airy function $\mathrm{Ai}(x)$. Then

$$\underset{\sim}{q}_{\nu,k} := \nu - a_k\left(\frac{\nu}{2}\right)^{1/3} < j_{\nu,k} < \nu - a_k\left(\frac{\nu}{2}\right)^{1/3} + \frac{3}{20}a_k^2\left(\frac{\nu}{2}\right)^{-1/3} =: \widetilde{q}_{\nu,k} \qquad \text{for all } \nu > 0 \text{ and } k \in \mathbb{N}. \tag{4.3}$$

Switching to existing bounds for $j'_{\nu,k}$, we note that although the McMahon asymptotic expansion for these zeros for a fixed ν and large k, similar to (4.1), is well-known, see [DLMF, (10.21.20)], we failed to find any analogues of (4.2) in this case. There is an analogue of the upper bound in (4.3): if

$$(0>)\,a'_1 > a'_2 > \dots$$

denotes the sequence of negative zeros of the derivative of the Airy function $\mathrm{Ai}'(x)$, then

$$j'_{\nu,k} < \nu + \left|a'_k\right|\left(\frac{\nu}{2} + \frac{8\left|a'_k\right|^{3/2}}{27}\right)^{1/3} + \frac{9\left|a'_k\right|^2}{10\times 2^{2/3}}\left(27\nu + 16\left|a'_k\right|^{3/2}\right)^{-1/3} =: \widetilde{\ell}'_{\nu,k} \qquad \text{for all } \nu \ge 0 \text{ and } k \in \mathbb{N},$$

which is obtained from [EL97], [E01, §1.7] after some manipulations required by the change of notation.

We compare these bounds to our bounds from Corollaries 1.6 and 1.12 numerically. The results of the computations are collated in Tables 1–3 in Appendix B. We note that all the calculations have been performed with 16 digit precision, and any differences between bounds not exceeding 10^{-16} are ignored. The inverse functions were evaluated using standard `Mathematica` routines with fixed precision.

The upper bound for $j_{\nu,k}$ obtained by using McMahon's expansions slightly outperforms our bound for low values of ν ($\lesssim 5$) and k ($\lesssim 100$), however even in the worst case $\nu = \frac{1}{2}$, $k = 1$, the relative deficiency of our bound is 7×10^{-4}. For a fixed ν and very large k, the bound $\widetilde{\ell}_{\nu,k}$ is theoretically better than our bound $\widetilde{j}_{\nu,k}$, however in practice the difference is negligible. Similarly, the Airy-type upper bound $\widetilde{q}_{\nu,k}$ should be theoretically better than our bound once one looks deep in the transition region, but in practice within the range of parameters we checked, it outperforms our bound only for very large ν and very small k ($k \lesssim 10$ for $\nu = 500000$), with the maximal relative deficiency of our bound being 3×10^{-4}: in all other cases our bound is better.

Elbert–Laforgia's lower bound $\underset{\sim}{\ell}_{\nu,k}$ generally outperforms our bound $\underset{\sim}{j}_{\nu,k}$ (as it is based on an additional term of the asymptotic expansion) but not by much, and is only valid for very low ν ($\lesssim 1$). The same observation as in the case of the upper bounds applies to Qu–Wang's lower bound: it becomes slightly more efficient than our bound only for very large ν and very small k.

Concerning the bounds for $j'_{\nu,k}$, there is no alternative lower bound to compare with; the upper bound $\widetilde{\ell}'_{\nu,k}$ only performs slightly better than our bound for very small k and very large ν.

Since accurately computing the large zeros of Bessel functions of large order and their derivatives is a non-trivial task, we do not compare our bounds to the actual values of these zeros; instead we plot, in Figures 12 and 13, the *maximal* possible errors by comparing our upper and lower bounds.

Acknowledgements

Research of NF was supported by the RSF grant 22-11-00092. Research of ML was partially supported by the EPSRC grants EP/W006898/1 and EP/V051881/1, and by the University of Reading RETF Open Fund. Research of IP was partially supported by NSERC.

References

[AB93] M. S. Ashbaugh and R. D. Benguria, *Universal bounds for the low eigenvalues of Neumann Laplacians in N dimensions*. SIAM J. Math. Anal. **24**:3 (1993), 557–570. doi: 10.1137/0524034. ☞ p. 20

[B17] J. Bremer, *On the numerical calculation of the roots of special functions satisfying second order ordinary differential equations*. SIAM J. Sci. Comput. **39**:1 (2017), A55–A82. doi: 10.1137/16M10571. ☞ p. 7

[B19] J. Bremer, *An algorithm for the rapid numerical evaluation of Bessel functions of real orders and arguments*. Adv. Comput. Math. **45** (2019), 173–211. doi: 10.1007/s10444-018-9613-9. ☞ p. 7

[BR16] J. Bremer and V. Rokhlin, *Improved estimates for nonoscillatory phase functions*. Discrete Contin. Dyn. Syst. Ser. A **36**:8 (2016), 4101–4131. doi: 10.3934/dcds.2016.36.4101. ☞ p. 7

[BFK16] D. Bucur, P. Freitas, and J. Kennedy, *The Robin problem*, in *Shape optimization and spectral theory*, A. Henrot (ed.). De Gruyter Open Poland, 2017. doi: 10.1515/9783110550887-004. ☞ p. 20

[DLMF] *NIST Digital Library of Mathematical Functions*. `https://dlmf.nist.gov/`, release 1.1.11 of 2023-09-15. F. W. J. Olver, A. B. Olde Daalhuis, D. W. Lozier, B. I. Schneider, R. F. Boisvert, C. W. Clark, B. R. Miller, B. V. Saunders, H. S. Cohl, and M. A. McClain (eds.). ☞ pp. 3, 5, 6, 14, 21, 25, and 26

[E01] Á. Elbert, *Some recent results on the zeros of Bessel functions and orthogonal polynomials*. J. Comput. Appl. Math. **133** (2001), 65–83. doi: 10.1016/S0377-0427(00)00635-X. ☞ pp. 6 and 26

[EL97] Á. Elbert and A. Laforgia, *An upper bound for the zeros of the derivative of Bessel functions*. Rend. Circ. Mat. Palermo **46**:1 (1997), 123–130. doi: 10.1007/BF02844477. ☞ pp. 6 and 26

[EL00] Á. Elbert and A. Laforgia, *Further results on McMahon's asymptotic approximations*. J. Phys. A **33**:36 (2000), 6333-6341. doi: 10.1088/0305-4470/33/36/305. ☞ pp. 6, 13, 14, and 25

[FLPS23] N. Filonov, M. Levitin, I. Polterovich, and D. A. Sher, *Pólya's conjecture for Euclidean balls*. Invent. Math. **234** (2023), 129–169. doi: 10.1007/s00222-023-01198-1. ☞ pp. 6, 8, and 11

[FLPS23a] N. Filonov, M. Levitin, I. Polterovich, and D. A. Sher, *Inequalities à la Pólya for the Aharonov–Bohm eigenvalues of the disk*. arXiv: 2311.14072. ☞ p. 6

[GG00] L. Gatteschi and C. Giordano, *Error bounds for McMahon's asympotic approximations of the zeros of the Bessel functions*. Integral Transforms Spec. Funct. **10**:1 (2000), 41–56. doi: 10.1080/10652460008819270. ☞ p. 6

[GG07] L. Gatteschi and C. Giordano, *On a method for generating inequalities for the zeros of certain functions*. J. Comput. Appl. Math. **207**:2 (2007), 186–191. doi: 10.1016/j.cam.2006.10.021. ☞ p. 6

[HBR15] Z. Heitman, J. Bremer, and V. Rokhlin, *On the existence of nonoscillatory phase functions for second order differential equations in the high-frequency regime*. J. Comput. Phys. **290** (2015), 1–27. doi: 10.1016/j.jcp.2015.02.028. ☞ p. 7

[HBRV15] Z. Heitman, J. Bremer, V. Rokhlin, and B. Vioreanu, *On the asymptotics of Bessel functions in the Fresnel regime*. Appl. Comput. Harmon. Anal. **39**:2 (2015), 347–356. doi: 10.1016/j.acha.2014.12.002. ☞ pp. 7, 13, and 21

[He70] H. W. Hethcote, *Bounds for zeros of some special functions*. Proc. Amer. Math. Soc. **25**:1 (1970), 72–74. doi: 10.2307/2036528. ☞ pp. 6, 14, and 25

[Ho17] D. E. Horsley, *Bessel phase functions: calculation and application*. Numer. Math. **136** (2017), 679–702. doi: 10.1007/s00211-016-0853-7. ☞ pp. 3, 5, 6, 7, 8, 10, and 13

[IS88] E. K. Ifantis and P. D. Siafarikas, *A differential equation for the positive zeros of the function* $\alpha J_\nu(z)+\gamma z J'_\nu(z)$. Z. Analysis Anwend. **7**:2 (1988), 195–192. doi: 10.4171/ZAA/295. ☞ p. 20

[L99] L. J. Landau, *Ratios of Bessel functions and roots of* $\alpha J_\nu(x) + x J'_\nu(x) = 0$. J. Math. Anal. Appl. **240**:1 (1999), 174–204. doi: 10.1006/jmaa.1999.6608. ☞ p. 20

[LMP23] M. Levitin, D. Mangoubi, and I. Polterovich, *Topics in Spectral Geometry*. Graduate Studies in Mathematics **237**. Amer. Math. Soc., Providence, RI, 2023. doi: 10.1090/gsm/237. ☞ p. 20

[LS94] L. Lorch and P. Szego, *Bounds and monotonicities for the zeros of derivatives of ultraspherical Bessel functions*. SIAM J. Math. Anal. **25**:2 (1994), 549–554. doi: 10.1137/S0036141092231 4. ☞ p. 20

[M94] J. McMahon, *On the roots of the Bessel and certain related functions*. Ann. Math. **9** (1894/1895), 23–30. doi: 10.2307/1967501. ☞ p. 25

[N21] G. Nemes, *Proofs of two conjectures on the real zeros of the cylinder and Airy functions*. SIAM J. Math. Anal. **53**:4 (2021), 4328–4349. doi: 10.1137/21M1396794. ☞ pp. 6 and 25

[O74] F. W. J. Olver, *Asymptotics and Special Functions*. Academic Press, Boston, 1974. doi: 10.1016/C2013-0-11254-8. ☞ pp. 8 and 22

[PA11] T. Pálmai and B. Apagyi, *Interlacing of positive real zeros of Bessel functions*. J. Math. Anal. Appl. **375** (2011), 320–322. doi: 10.1016/j.jmaa.2010.09.024. ☞ p. 3

[QW96] C. K. Qu and R. Wong, *"Best possible" upper and lower bounds for the zeros of the Bessel function* $J_\nu(x)$. Trans. Amer. Math. Soc. **351** (1999), 2833–2859. doi: 10.1090/S0002-9947-99-02165-0. ☞ pp. 6 and 25

[S23] D. A. Sher, *Joint asymptotic expansions for Bessel functions*. Pure Appl. Anal. **5**:2 (2023), 461–505. doi: 10.2140/paa.2023.5.461. ☞ pp. 6 and 8

[W95] G. N. Watson, *A treatise on the theory of Bessel functions*. Second edition. Cambridge Mathematical Library. Cambridge University Press, Cambridge, 1995. ☞ p. 25

Appendix A. Explicit expressions for some potentials

We have

$$\mathcal{V}_{\underset{\sim}{\theta}_\nu}(x) = \frac{q_\nu^{(1)}(x)}{q_\nu^{(2)}(x)}, \tag{A.1}$$

where

$$\begin{aligned} q_\nu^{(1)}(x) := \;& 4096x^{24} - 2048\left(24\nu^2 - 1\right)x^{22} + 128\left(2112\nu^4 - 128\nu^2 + 15\right)x^{20} \\ & - 32\left(28160\nu^6 - 1760\nu^4 - 584\nu^2 - 1\right)x^{18} \\ & + \left(2027520\nu^8 - 107520\nu^6 - 117376\nu^4 + 704\nu^2 + 1\right)x^{16} \\ & - 16\nu^2\left(202752\nu^8 - 7680\nu^6 - 13088\nu^4 + 223\nu^2 - 1\right)x^{14} \\ & + 16\nu^4\left(236544\nu^8 - 5376\nu^6 - 5000\nu^4 + 585\nu^2 + 6\right)x^{12} \\ & - 16\nu^6\left(202752\nu^8 - 2688\nu^6 + 11440\nu^4 + 935\nu^2 - 16\right)x^{10} \\ & + 16\nu^8\left(126720\nu^8 - 1920\nu^6 + 15272\nu^4 + 823\nu^2 + 16\right)x^8 \\ & - 128\nu^{12}\left(7040\nu^6 - 240\nu^4 + 808\nu^2 + 43\right)x^6 \\ & + 256\left(1056\nu^6 - 80\nu^4 + 17\nu^2 + 3\right)\nu^{14}x^4 \\ & - 1024\nu^{18}\left(48\nu^4 - 7\nu^2 - 5\right)x^2 + 1024\left(4\nu^2 - 1\right)\nu^{22}, \end{aligned} \tag{A.2}$$

and

$$q_\nu^{(2)}(x) := 64x^2\left(x^2 - \nu^2\right)^5\left(8x^6 + \left(1 - 24\nu^2\right)x^4 + 4\nu^2\left(6\nu^2 + 1\right)x^2 - 8\nu^6\right)^2. \tag{A.3}$$

Also,

$$\mathcal{V}_{\widetilde{\varphi}_\nu}(x) = \frac{q_\nu^{(3)}(x)}{q_\nu^{(4)}(x)}, \tag{A.4}$$

where

$$\begin{aligned} q_\nu^{(3)}(x) := \;& 4096x^{24} - 6144\left(8\nu^2+1\right)x^{22} + 128\left(2112\nu^4+320\nu^2-9\right)x^{20} \\ & - 32\left(28160\nu^6+2848\nu^4+760\nu^2+27\right)x^{18} \\ & + 3\left(675840\nu^8-3072\nu^6+46208\nu^4+448\nu^2+27\right)x^{16} \\ & - 16\nu^2\left(202752\nu^8-29184\nu^6+16352\nu^4+575\nu^2-27\right)x^{14} \\ & + 16\nu^4\left(236544\nu^8-69888\nu^6+10360\nu^4+1657\nu^2+54\right)x^{12} \\ & - 48\nu^6\left(67584\nu^8-29568\nu^6-1904\nu^4+533\nu^2-16\right)x^{10} \\ & + 16\nu^8\left(126720\nu^8-69504\nu^6-11480\nu^4+479\nu^2+16\right)x^8 \\ & - 128\nu^{12}\left(7040\nu^6-4272\nu^4-632\nu^2+5\right)x^6 \\ & + 768\nu^{14}\left(352\nu^6-208\nu^4-\nu^2+1\right)x^4 \\ & - 1024\nu^{18}\left(48\nu^4-23\nu^2+5\right)x^2 + 1024\left(4\nu^2-1\right)\nu^{22} \end{aligned} \tag{A.5}$$

and

$$q_\nu^{(4)}(x) := 64x^2\left(x^2-\nu^2\right)^5\left(8x^6-3\left(8\nu^2+1\right)x^4+4\left(6\nu^2-1\right)\nu^2x^2-8\nu^6\right)^2. \tag{A.6}$$

Finally,

$$\mathcal{V}_{\underset{\sim}{\psi}_{\nu,\eta}}(x) = \frac{q_{\mu,\eta}^{(5)}(x)}{q_{\mu,\eta}^{(6)}(x)}, \qquad \mu = \mu_{\nu,\eta}, \tag{A.7}$$

where

$$\begin{aligned} q_{\mu,\eta}^{(5)}(x) := \;& 16x^{16} \\ & - 32x^{14}\left(\eta^2+2\eta+4\mu^2\right) \\ & + 8x^{12}\left(3\eta^4+12\eta^3+\eta^2\left(28\mu^2+9\right)+6\eta\left(8\mu^2-1\right)+\left(56\mu^2-3\right)\mu^2\right) \\ & - 4x^{10}\left(2\eta^6+12\eta^5+12\eta^4\left(3\mu^2+2\right)+8\eta^3\left(15\mu^2+2\right)\right. \\ & \qquad \left.+14\eta^2\left(12\mu^2+5\right)\mu^2+12\eta\left(20\mu^2-1\right)\mu^2+\left(224\mu^2-31\right)\mu^4\right) \\ & + x^8\left(\eta^8+8\eta^7+8\eta^6\left(5\mu^2+3\right)+32\eta^5\left(6\mu^2+1\right)+2\eta^4\left(180\mu^4+145\mu^2+8\right)\right. \\ & \qquad +48\eta^3\left(20\mu^2+3\right)\mu^2+4\eta^2\left(280\mu^4+99\mu^2+6\right)\mu^2 \\ & \qquad \left.+8\eta\left(160\mu^2+13\right)\mu^4+20\left(56\mu^2-13\right)\mu^6\right) \\ & - \mu^2x^6\left(4\eta^8+24\eta^7+16\eta^6\left(5\mu^2+3\right)+32\eta^5\left(9\mu^2+1\right)+\eta^4\left(480\mu^2+293\right)\mu^2\right. \\ & \qquad +\eta^3\left(960\mu^4+76\mu^2\right)+4\eta^2\left(280\mu^4+56\mu^2+9\right)\mu^2 \\ & \qquad \left.+120\eta\left(8\mu^6+\mu^4\right)+56\left(16\mu^2-5\right)\mu^6\right) \\ & + \mu^4x^4\left(6\eta^8+24\eta^7+8\eta^6\left(10\mu^2+3\right)+192\eta^5\mu^2+9\eta^4\left(40\mu^2+11\right)\mu^2\right. \\ & \qquad +24\eta^3\left(20\mu^2-1\right)\mu^2+4\eta^2\left(168\mu^4+4\mu^2+3\right)\mu^2 \\ & \qquad \left.+24\eta\left(16\mu^2-1\right)\mu^4+32\left(14\mu^2-5\right)\mu^6\right) \\ & - \mu^6x^2\left(4\eta^8+8\eta^7+40\eta^6\mu^2+48\eta^5\mu^2+\eta^4\left(144\mu^2-1\right)\mu^2+4\eta^3\left(24\mu^2-5\right)\mu^2\right. \\ & \qquad \left.+8\eta^2\left(28\mu^2-3\right)\mu^4+8\eta\left(8\mu^2-5\right)\mu^4+4\left(32\mu^2-11\right)\mu^6\right) \\ & + \mu^8\left(\eta^4+4\eta^2\mu^2+4\mu^4-\mu^2\right)\left(\eta^2+2\mu^2\right)^2 \end{aligned} \tag{A.8}$$

and

$$q_{\mu,\eta}^{(6)}(x) := 4(x^2-\mu^2)^3x^2\left(2x^4-x^2\left((\eta+2)\eta+4\mu^2\right)+\mu^2\left(\eta^2+2\mu^2\right)\right)^2. \tag{A.9}$$

Appendix B. Numerical data

§B.1. Bounds for zeros of Bessel functions

Table 1: The comparison of our, Elbert–Laforgia's, and Qu–Wong's upper bounds for $j_{\nu,k}$. If $\widetilde{m}_{\nu,k} := \min\{\widetilde{j}_{\nu,k}, \widetilde{\ell}_{\nu,k}, \widetilde{q}_{\nu,k}\}$ denotes the best of the three bounds, the coloured entries in each row are those matching it. If $\widetilde{j}_{\nu,k} > \widetilde{m}_{\nu,k}$, the entry in the last column shows the relative deficiency of our bound.

ν	k	$\widetilde{j}_{\nu,k}$	$\widetilde{\ell}_{\nu,k}$	$\widetilde{q}_{\nu,k}$	$\frac{\widetilde{j}_{\nu,k}}{\widetilde{m}_{\nu,k}} - 1$
0	1	2.40810257797209	2.40924613788964		
	2	5.52043030619282	5.52052356422384		
	5	14.9309369836999	14.9309416805037		
	10	30.6346087249255	30.6346092684772		
	50	156.295034285583	156.295034289676		
	100	313.374266079643	313.374266080151		
	1000	3140.80729522508	3140.80729522508		
	10000	31415.1411417135	31415.1411417135		
	100000	314158.479961214	314158.479961214		
	500000	1570795.54139681	1570795.54139681		
$\frac{1}{2}$	1	3.14376279614743	3.14159265358979	3.27460318694968	7×10^{-4}
	2	6.28345002833208	6.28318530717959	7.05438435767338	4×10^{-5}
	5	15.7079800888803	15.7079632679490	20.5314460526698	1×10^{-6}
	10	31.4159286363346	31.4159265358979	47.7692005216613	7×10^{-8}
	50	157.079632696288	157.079632679490	368.663088373722	1×10^{-10}
	100	314.159265361079	314.159265358979	908.847335969838	7×10^{-12}
	1000	3141.59265358980	3141.59265358979	18983.1730584802	
	10000	31415.9265358979	31415.9265358979	406099.051081796	
	100000	314159.265358979	314159.265358979	8735498.79115534	
	500000	1570796.32679490	1570796.32679490	74666197.7784502	
1	1	3.83369791861688	3.83188486954530	3.88890738513848	5×10^{-4}
	2	7.01581736210639	7.01559818406170	7.40285121412499	3×10^{-5}
	5	16.4706452289041	16.4706302346712	19.2321654812515	9×10^{-7}
	10	32.1896818843079	32.1896799175785	42.2854077969397	6×10^{-8}
	50	157.862655418487	157.862655401933	304.378027137110	1×10^{-10}
	100	314.943472839851	314.943472837767	739.711587305586	7×10^{-12}
	1000	3142.37793241682	3142.37793241682	15150.0966962282	
	10000	31416.7119221250	31416.7119221250	322704.803661024	
	100000	314160.050755949	314160.050755949	6935149.13300128	
	500000	1570797.11219282	1570797.11219282	59267801.5559670	
5	1	8.77372338204280	8.83610697727954	8.77748993504362	
	2	12.3388145653858	12.3524627245014	12.3951530492719	
	5	22.2178113198726	22.2186275958908	22.7567429583036	
	10	38.1598700502104	38.1599260373733	40.6005910616904	
	50	164.072787945468	164.072787970360	216.371205491807	
	100	321.189319569572	321.189319568987	490.990987826608	2×10^{-12}
	1000	3148.65730681305	3148.65730681305	9115.22066902932	
	10000	31422.9947255486	31422.9947255486	189888.427570357	
	100000	314166.333903060	314166.333903060	4061112.22022502	
	500000	1570803.39537049	1570803.39537049	34675838.1018364	

ν	k	$\widetilde{j}_{\nu,k}$	$\widetilde{\ell}_{\nu,k}$	$\widetilde{q}_{\nu,k}$	$\frac{\widetilde{j}_{\nu,k}}{\widetilde{m}_{\nu,k}}-1$
10	1	14.4780593618721	14.8150624867862	14.4776533239189	3×10^{-5}
	2	18.4336923418614	18.5520743143216	18.4562220388682	
	5	28.8873862860562	28.9021354143944	29.1202550857628	
	10	45.2315754422830	45.2332565697875	46.3737266901699	
	50	171.711662928231	171.711665150058	201.823557261092	
	100	328.930191596730	328.930191681758	433.985076544903	
	1000	3156.49941795039	3156.49941795039	7418.61204821241	
	10000	31430.8475141856	31430.8475141856	151546.091220676	
	100000	314174.187765333	314174.187765334	3227144.69490720	
	500000	1570811.24932825	1570811.24932825	27533441.1155637	
50	1	57.1207457655499	62.0041045949062	57.1171076805129	6×10^{-5}
	2	62.8080187024269	66.0949975045479	62.8105158914088	
	5	76.4370860305146	77.8577326931975	76.4662469423382	
	10	95.8011096962304	96.3212070986120	95.9542784414793	
	50	229.362879678685	229.370990348625	235.332191927489	
	100	388.693660067007	388.694258337930	414.265541479911	
	1000	3218.95877848403	3218.95877849964	4923.29223763353	
	10000	31493.6412674832	31493.6412674832	91178.9720478066	
	100000	314237.015799664	314237.015799664	1898940.97658646	
	500000	1570874.08041742	1570874.08041742	16135766.4340724	
100	1	108.840879423458	120.880380157578	108.836246832758	4×10^{-5}
	2	115.739736248993	125.037089659834	115.740557472041	
	5	131.823950776853	137.202588450753	131.836011607965	
	10	153.900272851252	156.664768595604	153.962599154298	
	50	296.335776171518	296.471251735914	298.929907132201	
	100	459.529546576725	459.545645439361	471.533009349504	
	1000	3296.36998972096	3296.36999060841	4351.04720098391	
	10000	31572.0624063796	31572.0624063796	74207.6309465587	
	100000	314315.543686312	314315.543686312	1515506.03955682	
	500000	1570952.61784671	1570952.61784671	12831165.2167116	
1000	1	1018.67064844448	1180.40361331412	1018.66088584526	1×10^{-5}
	2	1032.76258530442	1184.62569023296	1032.76190059904	7×10^{-7}
	5	1064.24453144028	1197.25570362592	1064.24532031332	
	10	1104.92859950901	1218.18794810042	1104.93238865887	
	50	1328.95755863688	1380.97019620599	1329.09301911099	
	100	1548.25088464171	1575.19750272123	1548.90887404113	
	1000	4602.53426352435	4602.69406661919	4723.15283247506	
	10000	32970.7713584907	32970.7713673585	43521.6749153743	
	100000	315727.692643526	315727.692643526	742097.821357475	
	500000	1572366.01973148	1572366.01973148	6066913.80070566	
10000	1	10040.0498904506	11775.5007480898	10040.0290289155	2×10^{-6}
	2	10070.0511840226	11779.7297125815	10070.0495448888	2×10^{-7}
	5	10136.3963629401	11792.4129183083	10136.3963712851	
	10	10220.8123677153	11813.5393327241	10220.8126794286	
	50	10662.8217778127	11982.0061387084	10662.8309577604	
	100	11065.7962862662	12191.2634222777	11065.8362405931	
	1000	15491.7628369823	15760.5279241169	15498.3768788958	
	10000	46032.5838776516	46034.1806805361	47239.3537167537	
	100000	329714.785384131	329714.785472800	435227.952705537	
	500000	1586471.98808840	1586471.98808844	3063097.67857318	

ν	k	$\widetilde{j}_{\nu,k}$	$\widetilde{\ell}_{\nu,k}$	$\widetilde{q}_{\nu,k}$	$\frac{\widetilde{j}_{\nu,k}}{\widetilde{m}_{\nu,k}}-1$
100000	1	100086.203733327	117726.458311625	100086.158872022	4×10^{-7}
	2	100150.672924750	117730.687968554	100150.669387466	4×10^{-8}
	5	100292.921471816	117743.376569896	100292.921340968	1×10^{-9}
	10	100473.286256924	117764.523007627	100473.286274617	
	50	101406.591053031	117933.639180549	101406.591867126	
	100	102242.079713765	118144.896439004	102242.083055865	
	1000	110674.460043079	121922.018138173	110674.861526695	
	10000	154926.882893420	157613.832441531	154993.057404632	
	100000	460333.080262841	460349.047059410	472401.362824375	
	500000	1724975.77003468	1724975.79260235	2028908.15934764	
500000	1	500147.381239784	588619.602430817	500147.304554046	2×10^{-7}
	2	500257.570515678	588623.832149329	500257.564469154	1×10^{-8}
	5	500500.599560184	588636.521230963	500500.599326034	5×10^{-10}
	10	500808.554185199	588657.669454029	500808.554169543	3×10^{-11}
	50	502398.615413161	588826.844156947	502398.615572073	
	100	503817.163442824	589038.284846206	503817.164086853	
	1000	517891.863383625	592838.985093676	517891.932705137	
	10000	586230.238693899	630329.382318621	586239.210056145	
	100000	967172.336060185	972162.043475722	968798.233994082	
	500000	2301668.61976330	2301748.45319828	2362010.29220323	

Table 2: The comparison of our, Elbert–Laforgia's, and Qu–Wong's lower bounds for $j_{\nu,k}$. If $\underset{\sim}{m}_{\nu,k} := \max\left\{\underset{\sim}{j}_{\nu,k}, \underset{\sim}{\ell}_{\nu,k}, \underset{\sim}{q}_{\nu,k}\right\}$ denotes the best of the three bounds, the coloured entries in each row are those matching it. If $\underset{\sim}{j}_{\nu,k} < \underset{\sim}{m}_{\nu,k}$, the entry in the last column shows the relative deficiency of our bound.

ν	k	$\underset{\sim}{j}_{\nu,k}$	$\underset{\sim}{\ell}_{\nu,k}$	$\underset{\sim}{q}_{\nu,k}$	$\frac{\underset{\sim}{j}_{\nu,k}}{\underset{\sim}{m}_{\nu,k}}-1$
0	1	2.35619449019234	2.40307454796724		-2×10^{-2}
	2	5.49778714378214	5.52003775393840		-4×10^{-3}
	5	14.9225651045515	14.9309173864480		-6×10^{-4}
	10	30.6305283725005	30.6346064593785		-1×10^{-4}
	50	156.294234516092	156.295034268531		-5×10^{-6}
	100	313.373867195582	313.374266077528		-1×10^{-6}
	1000	3140.80725542640	3140.80729522508		-1×10^{-8}
	10000	31415.1411377345	31415.1411417135		-1×10^{-10}
	100000	314158.479960816	314158.479961214		-1×10^{-12}
	500000	1570795.54139673	1570795.54139681		-5×10^{-14}
$\frac{1}{2}$	1	3.10119764278657	3.14159265358979	1.97291537167673	-1×10^{-2}
	2	6.26321689238053	6.28318530717959	3.07524677778333	-3×10^{-3}
	5	15.7000008117865	15.7079632679490	5.50449056479522	-5×10^{-4}
	10	31.4119470742254	31.4159265358979	8.58162293766878	-1×10^{-4}
	50	157.078836900071	157.079632679490	24.4517345853548	-5×10^{-6}
	100	314.158867471034	314.159265358979	38.5846145963924	-1×10^{-6}
	1000	3141.59261380106	3141.59265358979	177.538763621880	-1×10^{-8}
	10000	31415.9265319191	31415.9265358979	822.364431896465	-1×10^{-10}
	100000	314159.265358581	314159.265358979	3815.31399222450	-1×10^{-12}
	500000	1570796.32679482	1570796.32679490	11155.0986540527	-5×10^{-14}

ν	k	$\widetilde{j}_{\nu,k}$	$\widetilde{\ell}_{\nu,k}$	$\widetilde{q}_{\nu,k}$	$\frac{\widetilde{j}_{\nu,k}}{\widetilde{m}_{\nu,k}}-1$
1	1	3.79443997608576	3.83149785113210	2.85575708148924	-1×10^{-2}
	2	6.99700190767405	7.01553182287974	4.24460762400316	-3×10^{-3}
	5	16.4629809123032	16.4706250109047	7.30526300658577	-5×10^{-4}
	10	32.1857886427175	32.1896792156545	11.1822068564821	-1×10^{-4}
	50	157.861863506199	157.862655395975	31.1772945855835	-5×10^{-6}
	100	314.943075932560	314.943472837017	48.9836076071283	-1×10^{-6}
	1000	3142.37789263802	3142.37793241682	224.054864934569	-1×10^{-8}
	10000	31416.7119181462	31416.7119221250	1036.48429790625	-1×10^{-10}
	100000	314160.050755551	314160.050755949	4807.36445023715	-1×10^{-12}
	500000	1570797.11219274	1570797.11219282	14054.9136473700	-5×10^{-14}
5	1	8.73567022436826		8.17329997222154	
	2	12.3227225053509		10.5482009934492	
	5	22.2113581058685		15.7818480787321	
	10	38.1564401016457		22.4113288086710	
	50	164.072024198901		56.6024478771247	
	100	321.188930139405		87.0508148429624	
	1000	3148.65726711332		386.418453827333	
	10000	31422.9947215707		1775.65324258109	
	100000	314166.333902662		8223.76760086749	
	500000	1570803.39537041		24036.8542936740	
10	1	14.4363906385824		13.9981074326327	
	2	18.4174021405972		16.9902952206943	
	5	28.8813543155782		23.5842773511631	
	10	45.2284209970154		31.9368996726856	
	50	171.710928343398		75.0150103064925	
	100	328.929810638849		113.377548781675	
	1000	3156.49937834850		490.557138795412	
	10000	31430.8475102086		2240.88329239253	
	100000	314174.187764936		10364.9983045269	
	500000	1570811.24932817		30288.2390926064	
50	1	57.0601473524213		56.8366675420313	
	2	62.7869087299433		61.9532366875564	
	5	76.4306643187313		73.2287875234740	
	10	95.7981975064759		87.5115707849523	
	50	229.362259920245		161.174103797040	
	100	388.693323896030		226.773121843061	
	1000	3218.95873962660		871.741148343930	
	10000	31493.6412635141		3864.75676983414	
	100000	314237.015799267		17756.7980286190	
	500000	1570874.08041734		51825.0605560830	
100	1	108.766857714791		108.613661347338	
	2	115.714556094408		115.060134517028	
	5	131.816671193838		129.266438364360	
	10	153.897155174351		147.261617646583	
	50	296.335198187589		240.070593577088	
	100	459.529237380598		322.720177265704	
	1000	3296.36995170726		1135.32897036330	
	10000	31572.0624024203		4906.29235454301	
	100000	314315.543685914		22409.1675624942	
	500000	1570952.61784663		65332.4886541907	

ν	k	$\underset{\sim}{j}_{\nu,k}$	$\underset{\sim}{\ell}_{\nu,k}$	$\underset{\sim}{q}_{\nu,k}$	$\frac{\underset{\sim}{j}_{\nu,k}}{\underset{\sim}{m}_{\nu,k}} - 1$
1000	1	1018.51756702735		1018.55757081489	-4×10^{-5}
	2	1032.71211855974		1032.44607624003	
	5	1064.23092084051		1063.05263006586	
	10	1104.92325532692		1101.82206856482	
	50	1328.95687010529		1301.77294585584	
	100	1548.25058086023		1479.83607607128	
	1000	4602.53423266599		3230.54864934569	
	10000	32970.7713546901		11354.8429790625	
	100000	315727.692643130		49063.6445023715	
	500000	1572366.01973140		141539.136473700	
10000	1	10039.7229535966		10039.9810743263	-3×10^{-5}
	2	10069.9441122528		10069.9029522069	
	5	10136.3679056193		10135.8427735116	
	10	10220.8014007353		10219.3689967269	
	50	10662.8204962035		10650.1501030649	
	100	11065.7957673197		11033.7754878167	
	1000	15491.7628066820		14805.5713879541	
	10000	46032.5838745664		32308.8329239253	
	100000	329714.785383751		113549.983045269	
	500000	1586471.98808833		312782.390926064	
100000	1	100085.500689806		100086.136613473	-6×10^{-6}
	2	100150.443003779		100150.601345170	-2×10^{-6}
	5	100292.860554032		100292.664383644	
	10	100473.262872899		100472.616176466	
	50	101406.588375922		101400.705935771	
	100	102242.078649619		102227.201772657	
	1000	110674.459991335		110353.289703633	
	10000	154926.882890391		148062.923545430	
	100000	460333.080262533		323091.675624942	
	500000	1724975.77003461		752324.886541907	
500000	1	500146.179459647		500147.291537168	-2×10^{-6}
	2	500257.177589753		500257.524677778	-7×10^{-7}
	5	500500.495512600		500500.449056480	
	10	500808.514273685		500808.162293767	
	50	502398.610860722		502395.173458535	
	100	503817.161639156		503808.461459639	
	1000	517891.863298728		517703.876362188	
	10000	586230.238689636		582186.443189646	
	100000	967172.336059901		881481.399222450	
	500000	2301668.61976324		1615459.86540527	

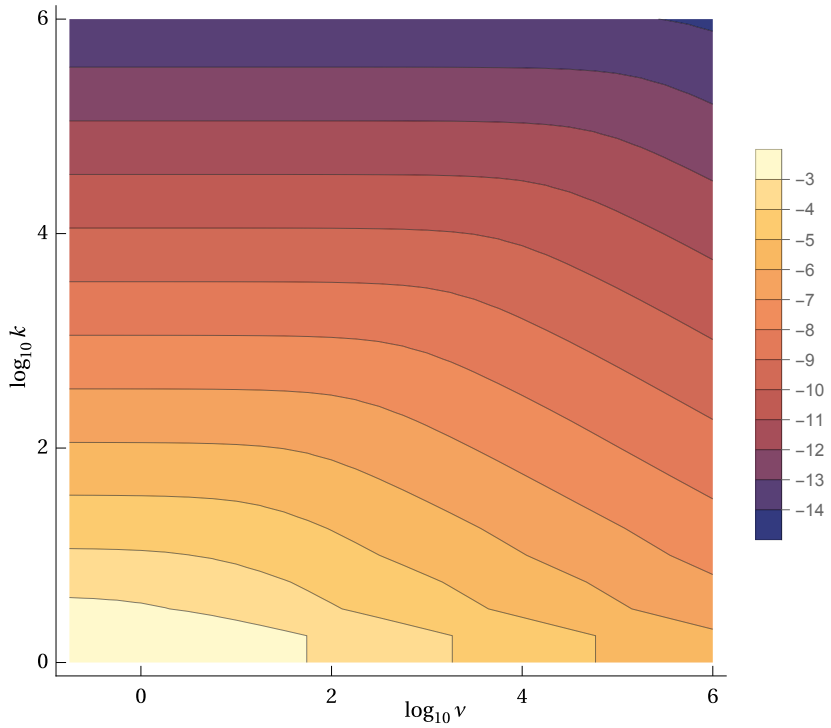

Figure 12: The contour plot of $\log_{10}\left(\frac{\widetilde{j}_{\nu,k}}{j_{\nu,k}}-1\right)$, which estimates from above the maximum possible order of relative error of our approximations of $j_{\nu,k}$.

§B.2. Bounds for zeros of derivatives of Bessel functions

Table 3: Our lower bound and the comparison of our and Elbert–Laforgia's upper bounds for $j'_{\nu,k}$. If $\widetilde{m}'_{\nu,k} := \min\left\{\widetilde{j}'_{\nu,k}, \widetilde{\ell}'_{\nu,k}\right\}$ denotes the best of the two upper bounds, the coloured entries in each row are those matching it. If $\widetilde{j}'_{\nu,k} > \widetilde{m}'_{\nu,k}$, the entry in the last column shows the relative deficiency of our bound.

ν	k	$\underset{\sim}{j}'_{\nu,k}$	$\widetilde{j}'_{\nu,k}$	$\widetilde{\ell}'_{\nu,k}$	$\frac{\widetilde{j}'_{\nu,k}}{\widetilde{m}'_{\nu,k}}-1$
	2	3.82905543678956	3.92699081698724	5.21994815723788	
	5	13.3236232806872	13.3517687777566	17.8482723692095	
	10	29.0468218553286	29.0597320457056	38.8629189129038	
	50	154.721014471994	154.723438189297	206.941758158503	
0	100	311.801868181958	311.803070868787	417.036190247476	
	1000	3139.23633964380	3139.23645909960	4198.72872262331	
	10000	31413.5703294702	31413.5703414077	42015.6503274934	
	100000	314156.909163295	314156.909164489	420184.866007090	
	500000	1570793.97060017	1570793.97060041	2100936.93567796	

ν	k	$\underset{\sim}{j'_{\nu,k}}$	$\widetilde{j}'_{\nu,k}$	$\widetilde{\ell}'_{\nu,k}$	$\frac{\widetilde{j}'_{\nu,k}}{\widetilde{m}'_{\nu,k}}-1$
$\frac{1}{2}$	1		1.48584693535690	1.52657094660980	
	2	4.60247860677616	4.68568659322651	5.84128905032192	
	5	14.1016664264204	14.1283185385025	18.4716385900913	
	10	29.8283630264584	29.8409412351793	39.4867451802621	
	50	155.505621002290	155.508032535003	207.565903087165	
	100	312.586869472825	312.588069144796	417.660372359456	
	1000	3140.02169802843	3140.02181745436	4199.35293773371	
	10000	31414.3557236548	31414.3557355921	42016.2745458797	
	100000	314157.694561061	314157.694562255	420185.490225804	
	500000	1570794.75599825	1570794.75599849	2100937.55989670	
1	1		2.11506214188671	2.11499393987502	3×10^{-5}
	2	5.33004070160281	5.40501381523099	6.45712461607948	
	5	14.8635367796392	14.8889705581512	19.0933165595504	
	10	30.6019171965764	30.6141946267452	40.1097896852094	
	50	156.288635764017	156.291035345361	208.189900476501	
	100	313.371074961794	313.372271647828	418.284481220551	
	1000	3140.80697683556	3140.80709623164	4199.97714556513	
	10000	31415.1411098817	31415.1411218186	42016.8987635385	
	100000	314158.479958031	314158.479959224	420186.114444445	
	500000	1570795.54139618	1570795.54139641	2100938.18411543	
5	1	6.28826192531053	6.65074326003913	6.54714840840174	2×10^{-2}
	2	10.5188417338511	10.5753107094334	11.2332989986105	
	5	20.5754812539651	20.5957954835809	24.0099702812020	
	10	36.5607736396374	36.5713809406576	45.0667270043476	
	50	162.498179300523	162.500490908179	213.176588124942	
	100	319.616768720740	319.617942511495	423.274719776078	
	1000	3147.08634964664	3147.08646880501	4204.97054621798	
	10000	31421.4239132894	31421.4239252240	42021.8924786219	
	100000	314164.763105141	314164.763106335	420191.108190953	
	500000	1570801.82457384	1570801.82457408	2100943.17786473	
10	1	11.6398057744632	12.0162638908975	11.8660736403637	1×10^{-2}
	2	16.4468248709150	16.4994512103844	16.9720812337165	
	5	27.1819924558840	27.1998893619366	30.0345337375884	
	10	43.6067615870698	43.6162303330504	51.1985421323618	
	50	170.135218972640	170.137436706410	219.396825169749	
	100	327.357136966911	327.358284407731	429.505960987985	
	1000	3154.92845527118	3154.92857413496	4211.21164225011	
	10000	31429.2767018707	31429.2767138023	42028.1345570098	
	100000	314172.616967415	314172.616968609	420197.350367542	
	500000	1570809.67853160	1570809.67853184	2100949.42005005	
50	1	52.8187848373174	53.3254083348661	53.0440529190390	5×10^{-3}
	2	60.0249962636869	60.0813194544867	60.2418339467916	
	5	74.3163203933786	74.3314682956021	75.7386724516605	
	10	93.9425695282024	93.9498510947580	98.4545059578280	
	50	227.750672604515	227.752470650764	268.662409540753	
	100	387.108315157524	387.109313313986	479.099715011984	
	1000	3217.38763707313	3217.38775367737	4261.11426459507	
	10000	31492.0704532998	31492.0704652076	42078.0685658962	
	100000	314235.445001727	314235.445002920	420247.287518400	
	500000	1570872.50962077	1570872.50962101	2100999.35748022	

ν	k	$\underset{\sim}{j}'_{\nu,k}$	$\widetilde{j}'_{\nu,k}$	$\widetilde{\ell}'_{\nu,k}$	$\frac{\widetilde{j}'_{\nu,k}}{\widetilde{m}'_{\nu,k}}-1$
100	1	103.552648845966	104.160029957632	103.803049301258	3×10^{-3}
	2	112.385101849666	112.448430986771	112.528002221252	
	5	129.358651207261	129.374174936818	130.325058224489	
	10	151.813259002596	151.820223347072	155.042104955214	
	50	294.664327855513	294.665911746948	329.158665247029	
	100	457.918838435071	457.919731860974	540.487440358064	
	1000	3294.79831773381	3294.79843173622	4323.42741287888	
	10000	31570.4915863354	31570.4915982138	42140.4795335826	
	100000	314313.972888315	314313.972889508	420309.708302353	
	500000	1570951.04705006	1570951.04705030	2101061.77913701	
1000	1	1007.65497214255	1008.87692662131	1008.10741918263	8×10^{-4}
	2	1025.97327758496	1026.08853535440	1026.00990668415	8×10^{-5}
	5	1059.53767346269	1059.56146481700	1059.76655932628	
	10	1101.19242597862	1101.20147226161	1102.01144720199	
	50	1326.56778093642	1326.56910593182	1338.72297124053	
	100	1546.19139906085	1546.19204915940	1582.10105006399	
	1000	4600.92489073707	4600.92497958265	5433.32953880577	
	10000	32969.1998239474	32969.1998353403	43262.6382055024	
	100000	315726.121837736	315726.121838924	421433.158077796	
	500000	1572364.44893452	1572364.44893476	2102185.34408437	
10000	1	10016.4918376026	10019.0850161927	10017.4305732935	2×10^{-4}
	2	10055.6275626539	10055.8663257080	10055.6423608815	2×10^{-5}
	5	10126.5382295259	10126.5852535008	10126.5888462274	
	10	10213.1216137128	10213.1385542345	10213.3033978649	
	50	10658.2856359516	10658.2876108152	10661.1849966748	
	100	11062.1238234066	11062.1246535611	11071.3066333350	
	1000	15489.7059732163	15489.7060377999	15852.5040437567	
	10000	46030.9746376957	46030.9746465753	54361.7461824340	
	100000	329713.213863324	329713.213864463	432654.745761900	
	500000	1586470.41726056	1586470.41726079	2113418.40311191	
100000	1	100035.530371101	100041.098972602	100037.536956311	4×10^{-5}
	2	100119.692630670	100120.202625833	100119.708964190	5×10^{-6}
	5	100271.813981416	100271.913355254	100271.825350454	9×10^{-7}
	10	100456.883755739	100456.919097553	100456.923246477	
	50	101397.105043612	101397.108914265	101397.740786006	
	100	102234.528924186	102234.530469187	102236.567493622	
	1000	110670.793673338	110670.793755672	110763.646675313	
	10000	154924.826290601	154924.826297055	158556.516370227	
	100000	460331.471036162	460331.471037050	543645.912187864	
	500000	1724974.19659187	1724974.19659209	2225491.96489915	
500000	1	500060.756008294	500070.272554347	500064.182433034	1×10^{-5}
	2	500204.624142480	500205.494863009	500204.649221081	2×10^{-6}
	5	500464.546806439	500464.716136887	500464.551147341	3×10^{-7}
	10	500780.557830912	500780.617909442	500780.571426180	9×10^{-8}
	50	502382.483279350	502382.489781183	502382.701278916	
	100	503804.363624797	503804.366193259	503805.063905356	
	1000	517885.834593690	517885.834718306	517918.417812500	
	10000	586227.229833856	586227.229841076	587665.712270748	
	100000	967170.501022458	967170.501023138	1017601.68651123	
	500000	2301667.01053780	2301667.01053798	2718242.20552639	

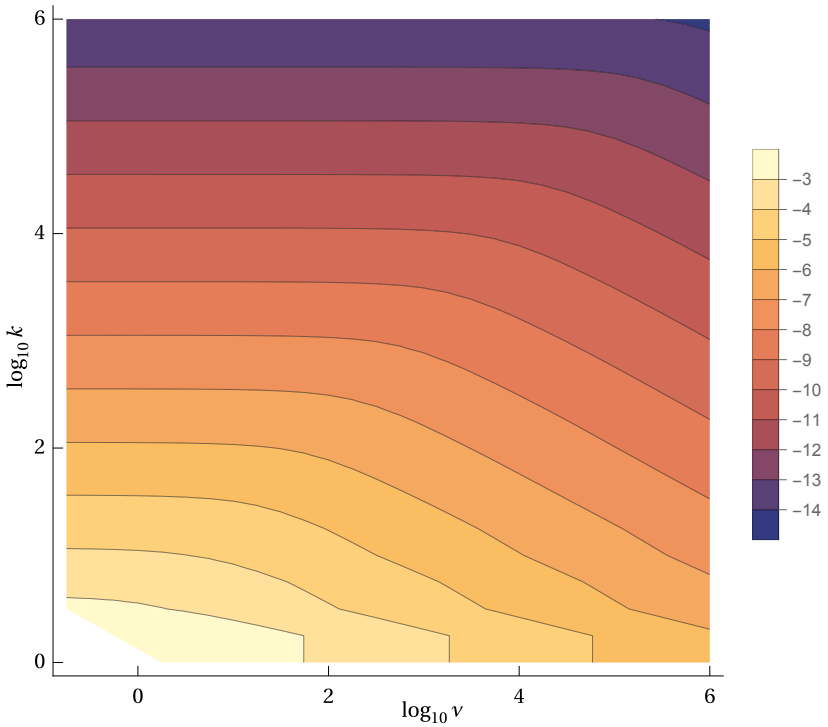

Figure 13: The contour plot of $\log_{10}\left(\frac{\tilde{j}'_{\nu,k}}{j'_{\nu,k}} - 1\right)$, which estimates from above the maximum possible order of the relative error of our approximations of $j'_{\nu,k}$.